

N81-26183

1. Report No. NASA CR-165709		2. Government Accession No.		3. Recipient's Catalog No.	
4. Title and Subtitle DEVELOPMENT OF ORTHOTROPIC BIREFRINGENT MATERIALS FOR PHOTOELASTIC STRESS ANALYSIS				5. Report Date May 1981	
				6. Performing Organization Code	
7. Author(s) I. M. Daniel, T. Niuro and G. M. Koller				8. Performing Organization Report No. M06044	
9. Performing Organization Name and Address IIT Research Institute 10 West 35th Street Chicago, Illinois 60616				10. Work Unit No.	
				11. Contract or Grant No. NAS-1-15541	
12. Sponsoring Agency Name and Address National Aeronautics and Space Administration Langley Research Center Hampton, Virginia 23665				13. Type of Report and Period Covered Contract Report Sept. 1978-Nov. 1980	
				14. Sponsoring Agency Code	
15. Supplementary Notes Langley Technical Monitor: Dr. Paul A. Cooper Final Report					
16. Abstract Materials were selected and fabrication procedures developed for orthotropic birefringent materials. An epoxy resin (Maraset 658/558 system) was selected as the matrix material. Fibers obtained from Style 3733 glass cloth and type 1062 glass roving were used as reinforcement. Two different fabrication procedures were used. In the first one, layers of unidirectional fibers removed from the glass cloth were stacked, impregnated with resin, bagged and cured in the autoclave at an elevated temperature. In the second procedure, the glass roving was dry-wound over metal frames, impregnated with resin and cured at room temperature under pressure and vacuum in an autoclave. Unidirectional, angle-ply and quasi-isotropic laminates of two thicknesses and with embedded flaws were fabricated. The matrix and the unidirectional glass/epoxy material were fully characterized. The density, fiber volume ratio, mechanical, and optical properties were determined. The fiber volume ratio was over 0.50. Birefringent properties were in good agreement with predictions based on a stress-proportioning concept and also, with one cexeption, with properties predicted by a finite element analysis.					
17. Key Words (Suggested by Author(s)) Birefringent composites Anisotropic photoelasticity Transparent composites Fabrication of glass/epoxy composites			18. Distribution Statement Unlimited		
19. Security Classif. (of this report) Unclassified		20. Security Classif. (of this page) Unclassified		21. No. of Pages 70	
				22. Price	

FOREWORD

This is the Final Report on IIT Research Institute Project No. M06044 (formerly D6161), "Development of Orthotropic Birefringent Materials for Photoelastic Stress Analysis," prepared by IITRI for NASA-Langley Research Center, under Contract No. NAS1-15541. The work described in this report was conducted in the period September 26, 1978 to November 15, 1980. Dr. Paul A. Cooper was the NASA-Langley Project Manager. Dr. I. M. Daniel of IITRI was the principal investigator. Additional contributions to the work reported herein were made by G. M. Koller and T. Nitro.

Use of commercial products or names of manufacturers in this report does not constitute official endorsement of such products or manufacturers, either expressed or implied, by the National Aeronautics and Space Administration.

TABLE OF CONTENTS

<u>Section</u>	<u>Page</u>
1. INTRODUCTION	1
2. ANISOTROPIC PHOTOELASTICITY	3
2.1 INTRODUCTION	3
2.2 MODEL MATERIALS	3
2.3 MATERIAL CHARACTERIZATION	5
3. MATERIAL DEVELOPMENT	10
4. FABRICATION OF BIREFRINGENT LAMINATES	16
4.1 UNIDIRECTIONAL LAMINATES	16
4.2 MULTIDIRECTIONAL LAMINATES	17
4.3 LAMINATES WITH EMBEDDED FLAWS	18
4.4 THICK LAMINATES	20
5. MECHANICAL AND OPTICAL CHARACTERIZATION	21
5.1 MATRIX RESIN	21
5.2 UNIDIRECTIONAL GLASS/EPOXY (MARASET/3733)	21
5.3 UNIDIRECTIONAL GLASS/EPOXY (MARASET/1062)	27
6. SUMMARY, CONCLUSIONS, AND RECOMMENDATIONS FOR FUTURE WORK	28
REFERENCES	30

LIST OF ILLUSTRATIONS

<u>Figure No.</u>		<u>Page</u>
1	Load-birefringence curve for $[0_{15}]$ glass/Maraset composite under uniaxial tensile loading. (Style 7500; Specimens 1 and 2)	32
2	Load-birefringence curve for $[90_{15}]$ glass/Maraset composite under uniaxial tensile loading. (Style 7500; Specimens 3 and 4)	33
3	Load-birefringence curve for $[45_{15}]$ glass/Maraset composite under uniaxial tensile loading. (Style 7500; Specimens 5 and 6)	34
4	Stress-strain curves for $[0_{15}]$ glass/Maraset composite under uniaxial tensile loading (Style 7500; Specimens 1 and 2).	35
5	Stress-strain curves for $[90_{15}]$ glass/Maraset composite under uniaxial tensile loading (Style 7500; Specimen 4).	36
6	Stress-strain curves for $[45_{15}]$ glass/Maraset composite under uniaxial tensile loading (Style 7500; Specimens 5 and 6).	37
7	Load-birefringence curve for $[0_{30}]$ glass/Maraset composite under uniaxial tensile loading (Style 3733; Specimen No. 42-1).	38
8	Load-birefringence curve for $[90_{30}]$ glass/Maraset composite under uniaxial tensile loading (Style 3733; Specimen No. 42-2).	39
9	Load-birefringence curve for $[45_{30}]$ glass/Maraset composite under uniaxial tensile loading (Style 3733; Specimen No. 42-3).	40
10	Stress-strain curves for $[0_{30}]$ glass/Maraset composite under uniaxial tensile loading (Style 3733; Specimen No. 42-1).	41
11	Stress-strain curves for $[90_{30}]$ glass/Maraset composite under uniaxial tensile loading (Style 3733; Specimen No. 42-2).	42
12	Stress-strain curves for $[45_{30}]$ glass/Maraset composite under uniaxial tensile loading (Style 3733; Specimen No. 42-3).	43
13	Cutting the glass fabric and removing fill fibers.	44

LIST OF ILLUSTRATIONS, Cont.

<u>Figure No.</u>		<u>Page</u>
14	Placing bundles of glass fibers over teflon film and pouring resin.	45
15	Placing glass bleeder layers and perforated teflon film over layup.	46
16	Sketch showing the arrangement of material layers employed in the fabrication of unidirectional birefringent laminates during the first stage of curing.	47
17	Composite layup with steel pressure plate and in vacuum bag before curing.	48
18	Removal of glass bleeder cloth after partial cure and application of teflon film.	49
19	Sketch showing the arrangement of material layers employed in the fabrication of angle-ply birefringent composite laminates during the first stage of curing.	50
20	Winding of glass roving over a single frame for unidirectional laminates.	51
21	Mounting of frame with 90-deg plies inside large frame and winding of 45-deg plies.	52
22	Winding of -45-deg plies over +45-deg and 90-deg plies.	53
23	Threading of glass roving around screw posts for outer 0-deg plies.	54
24	Layout of embedded flaws in birefringent laminates.	55
25	Winding with resin spread over it and covered with teflon sheet.	56
26	Layup with pressure plate in autoclave press.	57
27	Curing of laminates in blanket press autoclave.	58
28	Unidirectional $[0_8]$ glass/epoxy plate with embedded flaws (1062 glass roving; Maraset 658/558 epoxy).	59
29	Angle-ply $[\pm 45]_{2s}$ glass/epoxy plate with embedded flaws (1062 glass roving; Maraset 658/558 epoxy).	60

LIST OF ILLUSTRATIONS, Cont.

<u>Figure No.</u>		<u>Page</u>
30	Quasi-isotropic $[0/\pm 45/90]_S$ glass/epoxy plate with embedded flaws (1062 glass roving; Maraset 658/558 epoxy).	61
31	Stress-strain curves for Maraset 658/558 epoxy resin.	62
32	Stress-birefringence curve for Maraset 658/558 epoxy resin.	63
33	Stress-strain curves for $[0_{30}]$ glass/epoxy composite (Style 3733 glass; Maraset 658/558 epoxy).	64
34	Stress-strain curves for $[90_{30}]$ glass/epoxy composite (Style 3733 glass; Maraset 658/558 epoxy).	65
35	Stress-strain curves for $[45_{30}]$ glass/epoxy composite (Style 3733 glass; Maraset 658/558 epoxy).	66
36	Stress-birefringence curve for $[0_{30}]$ glass/epoxy composite (Style 3733 glass; Maraset 658/558 epoxy).	67
37	Stress-birefringence curve for $[90_{30}]$ glass/epoxy composite (Style 3733 glass; Maraset 658/558 epoxy).	68
38	Stress-birefringence curve for $[45_{30}]$ glass/epoxy composite (Style 3733 glass; Maraset 658/558 epoxy).	69
39	Stress-strain and stress-birefringence curves for $[0_{30}]$ glass/epoxy composite (Style 3733 glass; Maraset 658/558 epoxy).	70

LIST OF SYMBOLS

B_{ij}	= stress-optic photoelastic constants ($i, j = 1, 2, 6$ for orthotropic material under plane stress).
E_{11}, E_{22}	= moduli of unidirectional composite in fiber and transverse to the fiber direction, respectively.
E_{45}	= modulus of unidirectional composite at 45-deg to the fiber direction.
E_f, E_m	= moduli of fiber and matrix, respectively.
f	= stress fringe value of isotropic material.
f_{11}, f_{22}	= stress fringe values for unidirectional composite in fiber and transverse to the fiber direction, respectively.
f_{12}	= in-plane shear stress fringe value.
f_{45}	= stress fringe value at 45-deg with fiber direction.
f_x, f_y, f_{xy}	= stress fringe values for normal and shear stresses referred to x-y system.
f_θ	= stress fringe value at angle θ with the fiber direction.
f_f, f_m	= stress fringe values for fiber and matrix, respectively.
f_{11}^E, f_{22}^E	= strain fringe values in the fiber and transverse to the fiber directions, respectively.
f_{12}^E	= in-plane shear strain fringe value.
G_{12}	= in-plane shear modulus of unidirectional composite.
G_f, G_m	= shear modulus of fiber and matrix, respectively.
N	= birefringence (fringe order) per unit thickness.
N_{ij}	= birefringence tensor ($i, j = 1, 2$ for plane orthotropic material).
n	= fringe order.
p, q	= major and minor principal stresses in isotropic material on plane normal to direction of observation.
Q_{ij}	= stiffness tensor for unidirectional composite material ($i, j = 1, 2, 6$ for orthotropic material under plane stress).
S_{11T}, S_{22T}	= longitudinal and transverse tensile strength of unidirectional composite.

V_f, V_m = fiber volume and matrix volume ratio of composite, respectively.
 θ = angle from 1-direction (fiber direction).
 $\epsilon_{11}, \epsilon_{22}$ = normal strains in fiber and transverse to the fiber direction, respectively.
 ϵ_{45} = normal strain at 45-deg to loading axis.
 γ_{12} = in-plane shear strain.
 $\epsilon_{11T}^u, \epsilon_{22T}^u$ = ultimate longitudinal and transverse tensile strains, respectively.
 ν = Poisson's ratio of isotropic material.
 ν_{12}, ν_{21} = major and minor Poisson's ratio, respectively.
 ν_f, ν_m = fiber and matrix Poisson's ratio, respectively.
 $(\nu_{xy})_\theta$ = Poisson's ratio of θ -deg off-axis unidirectional composite.
 ρ_f, ρ_m, ρ_c = densities of fiber, matrix, and composite, respectively.
 σ_{11}, σ_{22} = normal stresses in the fiber and transverse to the fiber direction, respectively.
 τ_{12} = in-plane shear stress.
 $\sigma_x, \sigma_y, \sigma_{xy}$ = normal and shear stresses referred to x-y system.
 ϕ = isoclinic angle between principal material and principal birefringence axes.

1. INTRODUCTION

Photoelastic methods of stress analysis have been applied extensively to composite materials and structures. Two- and three-dimensional micromechanics studies have been conducted using scaled-up models of filamentary composites.^{1,2} Microphotoelastic experiments have been conducted utilizing models with prototype (boron) reinforcing filaments to closer simulate the three-dimensional state of stress and bond characteristics of the prototype composite.^{3,4} In macromechanical studies the photoelastic technique used most extensively is that of photoelastic coatings. These coatings, which can be applied directly to prototype (opaque) composite laminates, have been used successfully.^{5,8}

In recent years attempts have been made to combine the basic approach of photoelasticity with more realistic modeling of fibrous composite materials. Macromechanical stress analysis can be conducted by means of anisotropic photoelasticity using transparent birefringent composites. These materials are glass-fiber reinforced plastics with the matrix and the fibers having the same index of refraction. Transparent fibrous composites can be made to simulate the anisotropy of opaque fibrous composites such as boron/epoxy, graphite/epoxy, etc. These transparent composites can be treated as homogeneous materials with anisotropic elastic and optical properties.

Most of the research in this area has been conducted by a small number of investigators.⁹⁻²⁰ It has dealt primarily with measuring fringe values for a unidirectional material and developing stress- (or strain-) optic laws correlating the macroscopic state of stress (strain) with measured average birefringence.

The material for the anisotropic photoelastic studies above is not readily available and existing techniques produce materials with limitations in their mechanical and optical properties. The NASA-Langley Research Center, recognizing the need to develop optimized procedures and produce such material, has sponsored this program. The specific objective of this program was to develop, fabricate and deliver unidirectional and multi-ply transparent birefringent fibrous composite laminates.

The program consisted of the following tasks:

Task 1. Material Development

The objective of this task was to develop constituent materials and fabrication procedures to produce flat sheets of glass fiber reinforced composite with sufficient orthotropy, transparency and birefringence, such that they can be used for two-dimensional photoelastic analysis of orthotropic structures.

Task 2. Mechanical and Optical Characterization

The objective of this task was to determine the orthotropic mechanical and optical properties of the material developed.

Task 3. Fabrication of Laminates

The objective of this task was to fabricate birefringent composite laminates of the following layups: $[0_n]$; $[\pm 45]_{ns}$; $[0/\pm 45/90]_{ns}$.

Task 4. Fabrication of Birefringent Laminates with Embedded Flaws

The objective of this task was to develop techniques and fabricate birefringent composite laminates of $[0_n]$, $[\pm 45]_{ns}$ and $[0/\pm 45/90]_{ns}$ layups with embedded flaws.

Task 5. Fabrication of Thick Birefringent Laminates

The objective of this task was to develop techniques and fabricate birefringent composite laminates of $[0_{2n}]$, $[\pm 45]_{2ns}$ and $[0/\pm 45/90]_{2ns}$ layups and twice the thickness of those of Task 3.

2. ANISOTROPIC PHOTOELASTICITY

2.1 INTRODUCTION

Anisotropic photoelasticity (or photo-orthotropic elasticity as called by others) combines the basic approach of photoelasticity with more realistic modeling of the prototype fibrous composites. Some significant work has been conducted in the last few years by a small number of investigators.⁹⁻²⁰

The successful application of anisotropic photoelasticity has two important aspects, the preparation of suitable model materials and the development and application of the appropriate stress- (strain-) optic law.

2.2 MODEL MATERIALS

The basic requirements for a model material are that it be anisotropic, transparent and birefringent. The degree of anisotropy must be variable and adjustable to allow modeling of a variety of prototype composites. Transparency should be sufficient to allow viewing and recording of isochromatic fringes under transmitted polarized light. The material should have a low fringe value, i.e., it should be photoelastically sensitive. In addition to the optical requirements, the material should have a sufficiently high proportionality limit before it deforms nonlinearly or starts to fail. The material is basically a glass-fiber reinforced plastic with the glass fibers and the polymeric matrix having the same index of refraction.

The first known attempt to produce a transparent birefringent composite was described by Horridge.⁹ He used a Marco 28C resin (Scott Bader and Co.) and glass cloth and achieved a 0.50 fiber volume ratio. Because of the relatively high (for birefringent composites) fiber volume ratio, the fringe value was relatively high and it required the use of a compensator to measure fractional fringe orders. However, he reached the fifth or sixth fringe in simple tension for a 0.64 cm (1/4 in.) thick laminate.

Pih and Knight¹⁰ used a modified E-glass roving (W-1 glass by Owen-Corning Fiberglas, Inc. with a K895 finish). The matrix used was a room-temperature curing resin, Epon 815 (Shell Chemical Co.) cured with TETA and allyl glycidyl ether. The pot life of this resin system was a little too short (approximately

1-1/2 hours) to allow fabrication of large plates. The material was produced by winding resin-impregnated glass roving around a flat mandrel.

Sampson¹¹ produced a material of 0.40 fiber volume ratio by dry winding HTS glass roving and impregnating subsequently in vacuum with DER 332 resin cured with Hexahydrophthalic anhydride (Dow Chemical Co.). He achieved a close match of the two indices of refraction to 1.5490.

Dally and Prabhakaran¹² used glass fabric (Style 7500) containing E-glass fibers with a Volan finish. The matrix material was Paraplex P444A (Rohm and Haas Co.) polyester resin blended with 30 percent styrene to give an index of refraction equal to that of E-glass ($1.548 \pm .003$). The blend was cured with 0.5 percent benzoyl peroxide and 0.5 percent methyl ethyl ketone (MEK) peroxide. The fill fibers were removed from the glass fabric and then the glass was soaked in a resin bath. Laminates consisting of several resin-impregnated plies were rolled between two sheets of mylar to remove all entrapped air and placed between heavy plates to prevent re-entry of air. The curing cycle consisted of 2 hrs at 340 degK (153°F) and 4 hrs at 373 degK (212°F) under a pressure of 69 kPa (10 psi). The completed laminates consisted usually of 15 plies and were 1.91 mm (0.075 in.) thick. Thicker laminates are made by bonding thin ones together. Birefringent composites used at the IIT Research Institute were made by the same procedure above with satisfactory results.²⁰

Pipes and Rose¹⁴ attempted to produce an orthotropic model material. They used S-glass fibers stretched between alignment combs and impregnated with epoxy resin (PL-2, Photolastic, Inc.). However, they only achieved a fiber volume ratio of 0.03 and an anisotropy ratio of $E_{11}/E_{22} = 2.1$, where E_{11} and E_{22} are the moduli in the fiber and transverse to the fiber directions.

More recently Agarwal and Chaturvedi²¹ described the development of birefringent composites of improved transparency. They obtained an improved glass/polyester material by closely matching the indices of refraction of the fibers and the matrix and by controlling and minimizing the entrapped air.

From the discussion above, it appears that there are almost as many fabrication procedures as there are investigators in this field. There is, therefore, a need to review critically all known processes and improve them or develop new optimized procedures utilizing the best available constituent materials.

2.3 MATERIAL CHARACTERIZATION

The basic unidirectional material is mechanically and optically anisotropic. Mechanical behavior in the linear range is characterized by two moduli, two Poisson's ratios and an in-plane shear modulus.

E_{11} : in the fiber direction

E_{22} : transverse to the fiber direction

G_{12} : in-plane shear along the fibers

ν_{12} : major Poisson's ratio

ν_{21} : minor Poisson's ratio.

Birefringent behavior is described by three photoelastic constants f_{11} , f_{22} and f_{12} relating birefringence to longitudinal, transverse and in-plane shear stress, respectively.

Pih and Knight pioneered work in this area and developed a stress-optic law based upon a stress-proportioning technique.¹⁰ Later, Sampson formulated a stress-optic law which hypothesized the concept of a Mohr's circle of birefringence.¹¹ In addition, Sampson introduced the concept that three photoelastic constants are required in order to characterize these new materials photoelastically. Dally and Prabhakaran developed simple methods for the fabrication of the fiber-reinforced birefringent material, and predicted the three fundamental photoelastic constants based upon properties of the constituents.¹² Both experimental and theoretical results presented closely agreed with the stress-optic law formulated by Sampson. Bert has shown that the concept of a Mohr's circle of birefringence as proposed by Sampson, is a direct result of the tensorial nature of birefringence.¹³ Pipes and Rose expressed a strain-optic law based on one strain fringe value alone.¹⁴ Prabhakaran examined and verified Sampson's stress-optic law under biaxial stress conditions.¹⁵ He also identified a class of materials for which the simplified strain-optic law proposed by Pipes and Rose is a reasonable approximation.¹⁶ Cernosek recently showed the equivalence of Sampson's phenomenological theory and the stress-proportioning concept.¹⁷ He also showed that the optical isoclinic parameter can be predicted accurately, even in the presence of residual birefringence. More recently, Knight and Pih formulated general stress- and

strain-optic laws by using tensor forms of stress, birefringence and stress fringe values.¹⁸ These relations were then simplified to the more familiar two-dimensional equations. Stress distributions in composite laminates with complex geometries have been obtained by anisotropic photoelasticity.^{19,20}

The stress-optic law proposed by Sampson¹¹ is developed as follows:

The birefringence per unit thickness in an isotropic material is given by

$$N = \frac{p-q}{2f} \quad (1)$$

where p, q = major and minor principal stresses

f = fringe value.

The relation above, when referred to an arbitrary x-y system of coordinates, takes the form

$$N = \sqrt{\left(\frac{\sigma_x}{2f} - \frac{\sigma_y}{2f}\right)^2 + \left(\frac{2\tau_{xy}}{f}\right)^2} \quad (2)$$

Based on this form, Sampson postulated the following law for an orthotropic material:

$$N = \sqrt{\left(\frac{\sigma_x}{2f_x} - \frac{\sigma_y}{2f_y}\right)^2 + \left(\frac{2\tau_{xy}}{f_{xy}}\right)^2} \quad (3)$$

which involves three different material fringe values, f_x , f_y and f_{xy} .

In an anisotropic material, in general we can define and distinguish four sets of principal axes: principal material axes along which the modulus has maximum and minimum values; principal stress axes where the stresses reach maximum and minimum values; principal strain axes where the strains reach maximum and minimum values; and principal birefringence (or optical) axes where the components of birefringence reach maximum and minimum values. These sets of axes do not have to coincide, in general.

If the x-y system is assumed to coincide with the principal material axes of the orthotropic material (fiber and transverse to the fiber directions of a unidirectional composite), the components of birefringence

$$\begin{aligned}
N_{11} &= \frac{\sigma_{11}}{2f_{11}} \\
N_{22} &= \frac{\sigma_{22}}{2f_{22}} \\
N_{12} &= \frac{\tau_{12}}{f_{12}}
\end{aligned} \tag{4}$$

follow the same transformation relations as the corresponding stress components.

Thus, an orthotropic material can be fully characterized optically by determining the fringe values f_{11} , f_{22} and f_{12} . The first two values can be easily determined by testing tensile coupons, say in 0-deg and 90-deg directions with respect to the fibers, as described previously. The value of f_{12} requires a pure shear test which is not easy to conduct. However, it can be computed from the values of f_{11} , f_{22} and f_{45} , the latter being determined from a tensile coupon at 45-deg to the material axes.

From considerations of equilibrium and stress-transformation relations, Equation 3 yields

$$f_{\theta} = f_{11} \left[(\cos^2 \theta - \frac{f_{11}}{f_{22}} \sin^2 \theta)^2 + \frac{4f_{11}^2}{f_{12}^2} \sin^2 2\theta \right]^{-1/2} \tag{5}$$

where θ is the angle between the principal stress p and the 1-direction. By determining f_{11} , f_{22} and f_{45} , Equation 5 can be solved for f_{12} by substituting $\theta = 45^\circ$.

In introducing the tensorial nature of birefringence, Bert¹³ proposed that the general unidirectional fiber-reinforced composite material could be considered similar to an orthorhombic crystal which possesses three principal material directions. Thus, the components of the birefringence tensor N_{ij} are related to the stress components in the lamina coordinate system as follows:

$$\begin{aligned}
N_{11} &= B_{11}\sigma_{11} + B_{12}\sigma_{22} + 0\tau_{12} \\
N_{22} &= B_{21}\sigma_{11} + B_{22}\sigma_{22} + 0\tau_{12} \\
N_{12} &= 0\sigma_{11} + 0\sigma_{22} + B_{66}\tau_{12}
\end{aligned} \tag{6}$$

where the B_{ij} are photoelastic constants.

The familiar stress-optic coefficients can be expressed in terms of the photoelastic constants, B_{ij} .

$$\begin{aligned} f_{11} &= \frac{1}{2(B_{11} - B_{21})} \\ f_{22} &= \frac{1}{2(B_{22} - B_{12})} \\ f_{12} &= \frac{1}{B_{66}} \end{aligned} \quad (7)$$

The isoclinic angle is given by

$$\tan 2\phi = \frac{-2B_{66}\tau_{12}}{(B_{11} - B_{21})\sigma_{11} - (B_{22} - B_{12})\sigma_{22}} = \frac{-4\tau_{12}/f_{12}}{\sigma_{11}/f_{11} - \sigma_{22}/f_{22}} \quad (8)$$

The strain-optic law may be derived from the stress-optic law through substitution of the constitutive relations into Equation 3. This does not imply any hypothesis regarding the physical origin of birefringence, but simply recognizes the fact that the stress, strain and birefringent tensors are inter-related mathematically.

An orthotropic material under plane stress is characterized by the following constitutive relationships:²²

$$\begin{aligned} \sigma_{11} &= Q_{11}\epsilon_{11} + Q_{12}\epsilon_{22} \\ \sigma_{22} &= Q_{12}\epsilon_{11} + Q_{22}\epsilon_{22} \\ \tau_{12} &= Q_{66}\gamma_{12} \end{aligned} \quad (9)$$

where Q_{ij} are the material stiffness constants and the stresses and strains are referred to the principal material axes.

The strain-optic coefficients f_{11}^E , f_{22}^E and f_{12}^E are given in terms of the stress-optic coefficients and the material stiffness constants Q_{ij} .

$$f_{11}^{\epsilon} = \frac{f_{11}f_{22}}{f_{22}Q_{11} - f_{11}Q_{12}}$$

$$f_{22}^{\epsilon} = \frac{f_{11}f_{22}}{f_{11}Q_{22} - f_{22}Q_{12}} \quad (10)$$

$$f_{12}^{\epsilon} = \frac{f_{12}}{2Q_{66}}$$

The isoclinic angle may, therefore, be related to the strain components and strain optic coefficients as follows:

$$\tan 2\phi = \frac{2\gamma_{12}/f_{12}}{[\epsilon_{11}/f_{11}^{\epsilon} - \epsilon_{22}/f_{22}^{\epsilon}]} \quad (11)$$

3. MATERIAL DEVELOPMENT

Materials and processes used to date by various investigators, including the writer, were reviewed critically. Mechanical and optical limitations of available materials were studied and guidelines for improvement established.

The major requirements for a matrix resin are the following:

- (1) It should be transparent when cured and amenable to small variations in the index of refraction.
- (2) It should have a sufficiently long pot life, i.e., 4 to 6 hours.
- (3) It should be curable at or near room temperature with minimum shrinkage, so as to minimize initial birefringence.
- (4) It should have sufficient birefringent sensitivity, i.e., a low material fringe value.

The following matrix materials were considered:

- (1) Epon 815, cured with various amounts of amine hardeners, such as DETA or TETA.
- (2) DER 332 epoxy cured with HHPA. This resin can also be cured with DETA and modified (plasticized) by mixing it with DER 732.
- (3) Polyester resins such as Paraplex P444A blended with styrene.
- (4) Maraset 658/558 epoxy resin (Marblette Corp.).
- (5) Ciba 502 resin with Type 956 hardener.

Preliminary tests with DER 332 (Dow Epoxy Resin) cured with 75 phr HHPA (hexahydrophthalic anhydride) showed that the material has a very long pot life. It takes more than two days to gel at 373°K (212°F). Curing was accelerated by adding approximately one percent of TETA (Triethylene Triamine) or DEH 24. However, the addition of the accelerator makes the otherwise white resin yellowish. Epon 815 was found to yield somewhat darker castings.

Experiments with polyesters yielded satisfactory sheets, but they required relatively high temperatures for curing and postcuring (342°K, 155°F; and 373°K, 212°F).

The Maraset resin system was found the most satisfactory. The basic resin, Maraset 658, is mixed with the hardener, Maraset 558, in a 2:1 ratio by weight. The resin and hardener are heated to 325°K (125°F) and mixed. The resin has a pot life of several hours and cures at room temperature with a minimum amount of shrinkage. The casting is water clear. It has an index of refraction very close to that of E-glass (1.548).

The availability of suitable glass fibers was investigated. Owens Corning Fiberglass and PPG Industries were contacted. The W-1 single-end yarn with P678 or K895 finishes is no longer available. Preliminary tests with available glass rovings having a silane binder resulted in opaque samples. A quantity of glass roving without any finish was received from Owens Corning Fiberglass. Several samples were prepared using this roving and three types of resin matrix, DER 332, Maraset 658/558 and Paraplex P444-A. In all cases the transparency was unsatisfactory, probably because of poor wetting of the bare glass roving.

In the absence of suitable glass roving, a quantity of glass fabric of Style 7500 with Volan finish was obtained from J. P. Stevens and Co. The Volan finish is a methacrylate chromium complex applied to the glass fabric after burning off the silane finish. Layers of unidirectional glass fibers were obtained from the glass cloth above by pulling out the fill fibers.

Unidirectional glass/epoxy laminates were prepared using fibers from the glass cloth above impregnated with Maraset 658/558 resin system. Layers of unidirectional fibers were held together by tape at their ends and stapled to wooden strips. The fibers were stretched slightly in a frame made of these wooden strips and two threaded rods. Initially, fifteen layers of glass fibers were stretched over the frame and the frame mounted over the bottom part of the mold. Resin was poured over the glass fibers until they were completely covered. The open face mold was then placed in a vacuum oven where vacuum was drawn for approximately 30 min. at 311°K (100°F). Then, the laminate was covered with a teflon film stretched over it and the mold cover plate. Pressure was applied in a variety of ways, mechanically through clamps; by bagging the layup and applying vacuum; or by applying external pressure in an autoclave.

Specimens for development of optimum fabrication parameters were 12.7 cm x 22.9 cm (5 in. x 9 in.) 15 to 20-ply thick. The three most important criteria used at this stage were transparency, thickness uniformity and absence of air bubbles. A number of specimens was prepared, some of which were very satisfactory.

One of the initial 15-ply laminates was used for preliminary determination of optical and mechanical properties. The laminate was approximately 2.41 mm (0.095 in.) thick. Coupons were machined from this laminate at 0-, 90- and 45-deg to the fiber direction. These coupons were nominally 2.54 cm (1 in.) wide with lengths varying from 12.7 cm to 22.9 cm (5 in. to 9 in.). Two coupons of each of the three fiber orientations were tabbed and loaded in tension in the polariscope. Birefringent measurements were made at each of several load levels. Photoelastic results for six coupons are shown in Figures 1 to 3. The material fringe values obtained from these tests are:

$$f_{11} = 41.0 \text{ kPa-m/fr (234 psi-in./fr)}$$

$$f_{22} = 19.3 \text{ kPa-m/fr (110 psi-in./fr)}$$

$$f_{45} = 18.1 \text{ kPa-m/fr (103 psi-in./fr)}$$

The laminate had a residual birefringence of 0.43.

Another set of coupon specimens, two each for the 0-, 45- and 90-deg fiber directions, were instrumented with strain gages and loaded in tension. Stress-strain curves are shown in Figures 4 to 6. Mechanical properties determined from these curves are:

$$E_{11} = 19.4 \text{ GPa (2.81} \times 10^6 \text{ psi)}$$

$$E_{22} = 7.1 \text{ GPa (1.03} \times 10^6 \text{ psi)}$$

$$E_{45} = 7.0 \text{ GPa (1.02} \times 10^6 \text{ psi)}$$

$$\nu_{12} = 0.33$$

$$\nu_{21} = 0.12$$

$$(\nu_{xy})_{\theta=45^\circ} = 0.36.$$

The ratio of the longitudinal to the transverse modulus is 2.73 which is lower than the desired one of at least 4. Attempts were made to increase the glass content or, equivalently, to reduce the laminate thickness for the same amount of glass.

The J. P. Stevens and Co. was contacted regarding additional supplies of glass cloth with Volan finish. It was found that this finish is no longer available. However, two new finishes are supplied with their glass fabrics. Finish S-910 is an ultra high performance finish compatible with polyester resins. Finish S-920 is a similar one for epoxy resins. Large quantities of glass fabric of Style 7500 with S-920 finish and Style 3733 with S-910 finish were obtained.

A large number of samples were prepared using fibers from these two fabrics with three types of matrix resins: DER 332, Maraset 658/558 and Paraplex P444-A. Of the three resin systems, Maraset 658/558 produced the clearest laminates. Of the two glass fabrics, Style 3733 seems to give slightly better results because the fibers are not twisted like those of Style 7500 and, therefore, they wet better and are less prone to entrap air.

A second laminate made of 30 plies of Style 3733 glass and Maraset resin was selected for preliminary mechanical and optical characterization. The glass was prepared by pulling out the fill fibers from the fabric as before. The resin was brushed over the glass plies until they were all wetted. Then, the layup was covered with 0.025 mm (0.001 in.) thick Teflon sheets on both sides and the entrapped air squeezed out with a roller. Subsequently, the laminate was bagged, vacuum was drawn, and a pressure of 138 kPa (20 psi) was applied in the autoclave. Then, the vacuum was cut off and the bag allowed to vent to atmosphere while still under pressure. Curing was completed at room temperature under pressure. The resulting thickness was $t = 2.54 \pm 0.13$ mm (0.100 ± 0.005 in.). The transparency was good and the surfaces smooth. Three coupons, 2.54 cm (1 in.) wide and 15.24 cm (6 in.) long, were machined from this laminate, tabbed with glass/epoxy tabs and instrumented with strain gages. They were then loaded in tension in steps. Photoelastic and strain gage readings were taken at each load level.

Photoelastic results for these specimens are shown in Figures 7, 8, and 9. The material fringe values obtained from these tests are:

$$f_{11} = 58.4 \frac{\text{kPa-m}}{\text{fr}} (333 \frac{\text{psi-in.}}{\text{fr}})$$

$$f_{22} = 29.6 \frac{\text{kPa-m}}{\text{fr}} (169 \frac{\text{psi-in.}}{\text{fr}})$$

$$f_{45} = 30.8 \frac{\text{kPa-m}}{\text{fr}} (176 \frac{\text{psi-in.}}{\text{fr}})$$

The laminate had a residual birefringence of 0.45. The results above show that this laminate is appreciably less sensitive photoelastically than the laminate with the Style 7500 glass, although the latter contained only a slightly lower quantity of glass by weight.

Stress-strain curves for the same laminate above are shown in Figures 10, 11 and 12. Moduli and Poisson's ratios determined from these tests are:

$$E_{11} = 26.9 \text{ GPa } (3.90 \times 10^6 \text{ psi})$$

$$E_{22} = 7.5 \text{ GPa } (1.08 \times 10^6 \text{ psi})$$

$$E_{45} = 7.8 \text{ GPa } (1.13 \times 10^6 \text{ psi})$$

$$\nu_{12} = 0.34$$

$$\nu_{21} = 0.07$$

$$(\nu_{xy})_{\theta=45^\circ} = 0.44.$$

The ratio of the longitudinal to the transverse modulus is 3.61, which is appreciably higher than before, but still under the desired value of 4. The longitudinal modulus for 30 plies of Style 3733 glass is appreciably higher than that for 15 plies of Style 7500 glass although the former contained only a little more glass than the Style 7500 laminate.

Experiments were continued for the development of a satisfactory laminate fabrication process. Large plates 33 cm x 33 cm (13 in. x 13 in.) were prepared with Styles 7500 and 3733 glass using the Maraset 658/558 resin system. In both cases clear laminates with smooth surfaces were obtained. The first group of specimens was prepared with 20 layers of Style 7500 glass with S-920 finish. The resulting thicknesses ranged between 2.67 mm (0.105 in.) and 3.56 mm (0.140 in.). A second series of plates was prepared using 30 layers of Style 3733 glass with S-910 finish. Several modifications were introduced in the fabrication procedure in order to obtain thinner laminates with higher glass content. More resin was squeezed through the ends of the plate by

rolling more vigorously between the teflon sheets; strips of glass cloth were added at the ends to soak excess resin; special cavities were provided at the ends in the mold to hold excess resin; the curing pressure was increased to 656 kPa (95 psi). The average thickness of these plates was 2.72 mm (0.107 in.) which was judged unsatisfactory because of the low glass content (less than 50 percent).

A different method for drawing out excess resin from the layup was investigated. The applicability of using bleeder plies as in conventional autoclave curing of prepreg layups was investigated. Several 15.2 cm x 25.4 cm (6 in. x 10 in.) specimens were prepared for this purpose. The matrix resin was poured over the fibers divided into three batches of 10 layers each. The layup was placed over a teflon sheet and covered with a separator sheet and several plies of 1581 glass cloth. The layup was then bagged and partially cured in the autoclave under vacuum and pressure. After partial cure, the glass cloths with the separator were removed and replaced with a teflon sheet. The laminate was rebagged and cured under pressure at an elevated temperature. The purpose of the second stage of curing was to smooth out the rough imprint of the separator on the top surface of the plate. Several curing parameters were investigated, i.e., duration, vacuum, pressure and temperature of first and second stages of cure.

In the final stages of the program a new process was developed for laminate fabrication. Type 1062 glass roving was obtained from PPG Industries. This roving was dry-wound on an open metal frame in a filament winding machine. The detailed fabrication procedure is discussed later in this report. Different types of frames were used to produce unidirectional and multidirectional windings. The matrix resin is poured in two halves on each side of the fiber layup and spread over the surface as uniformly as possible. The wet layup is covered on both sides by two teflon sheets and placed in a blanket press between two thick steel pressure plates. The assembly is then covered with a vent glass cloth and the blanket. Vacuum is drawn for approximately thirty minutes and the layup is cured under pressure at room temperature. This fabrication procedure resulted in satisfactory transparent laminates with embedded flaws. Satisfactory laminates up to 0.508 cm (0.200 in.) thick were fabricated.

4. FABRICATION OF BIREFRINGENT LAMINATES

4.1 UNIDIRECTIONAL LAMINATES

Following all preliminary development and testing described heretofore, a general procedure was adopted for fabrication of unidirectional birefringent glass/epoxy plates. Style 3733 glass cloth with S-910 finish was used as the source of the reinforcing fibers. Maraset 658/558 epoxy system was used as matrix. The glass cloth was cut in rectangular 41.9 cm x 33.0 cm (16.5 in. x 13 in.) pieces using 2.54 cm (1 in.) masking tape to hold the ends of the warp fibers together while removing the fill fibers (Figure 13). Reasonable care must be taken to avoid disturbing the fibers because this cloth is relatively fragile and is subject to fraying. It was selected because it has no noticeable twist. The unidirectional glass layers were then arranged in bundles of ten, stapled together at the taped ends to facilitate handling. A quantity of 180 g Maraset 658 resin was heated in a beaker to 317°K (110°F), then mixed with a quantity of 90 g Maraset 558 hardener and degassed for approximately three minutes.

A bundle of ten layers of glass fibers was placed over a 0.051 mm (0.002 in.) thick FEP teflon film. Approximately one-third of the resin was poured over it and spread with a spatula working the resin into the fibers (Figure 14). The fibers were kept stretched and straightened during wetting with the resin. Then, the next bundle of fiber layers was placed on top of the first one and another third of the total resin was poured and spread over it. The operation was repeated with the third bundle and the remaining resin.

The wet layup with the teflon film was placed over a 34.3 cm x 40.6 cm x 1.91 cm (13.5 in. x 16 in. x 0.75 in.) steel plate lined with 3.17 mm x 6.35 mm (1/8 in. x 1/4 in.) Corprene dam along two edges. On top of the layup were placed in succession a layer of TX 1040 separator (teflon coated glass scrim cloth), three plies of 1581 glass bleeder cloth, a 0.051 mm (0.002 in.) thick teflon film perforated on 5 cm (2 in.) centers and one ply 1581 glass cloth acting as a vent for drawing vacuum (Figures 15 and 16). This assembly was then covered with a 33 cm x 33 cm x 1.91 cm (13 in. x 13 in. x 0.75 in.) steel pressure plate which in turn was covered with glass cloth buffer to prevent tearing of the vacuum bag over the sharp corners of this plate (Figure 17).

The autoclave was pre-heated to a temperature of 325°K (125°F). The assembled layup was vacuum-bagged over the heating plate of the autoclave with a Capran film (nylon film by Allied Chemical) sealed with Presstite (Figure 17). Full vacuum was drawn and a pressure of 690 kPa (100 psi) was applied. After 15 minutes, the vacuum was cut off and the bag allowed to vent to atmosphere while still under pressure. The plate was partially cured for one hour. Afterwards, it was removed from the autoclave and placed in a freezer for approximately five minutes. When the resin became firm enough, the separator and glass bleeder layers were removed and replaced with a 0.051 mm (0.002 in.) thick teflon film (Figure 18). The layup was re-bagged and postcured in the autoclave under vacuum and 690 kPa (100 psi) pressure at 342°K (155°F) for one hour. The purpose of this second stage of curing was to smooth out the imprint of the separator layer on the top surface of the glass/epoxy plate.

The procedure above was followed in the fabrication of ten 33 cm x 33 cm (13 in. x 13 in.) unidirectional glass/epoxy plates. The nominal thickness was 0.203 cm (0.80 in.). (These plates were designated as 200 series.)

4.2 MULTIDIRECTIONAL LAMINATES

The procedure discussed before was modified for the fabrication of multidirectional laminates. Two sets of specimens were fabricated of the following layups: $[+45_4/-45_4]_{2S}$ and $[0_4/+45_4/-45_4/90_4]_S$. The specimens are 32 plies thick and made up by stacking groups of four unidirectional glass layers at the various orientations. The glass fiber bundles were strung over a 1.91 cm (0.75 in.) thick plywood plate with a 35 cm x 35 cm (13.75 in. x 13.75 in.) square cutout covered first with a 0.051 mm (0.002 in.) thick teflon film. In this case, 300 g of mixed resin and hardener were poured over the glass fibers from the top and spread out as uniformly as possible. On top of the layup were placed in succession a layer of TX1040 separator (teflon coated glass scrim cloth), two plies of 1581 glass bleeder cloth, a 0.051 mm (0.002 in.) thick teflon film perforated on 5 cm (2 in.) centers and one ply 1581 glass cloth acting as a vent for drawing vacuum (Figure 19). A 1.91 cm (0.75 in.) thick 33 cm x 33 cm (13 in. x 13 in.) steel plate was placed underneath the layup in the cutout of the plywood plate. The assembly was then covered with another steel pressure plate of the same dimensions above which, in turn, was covered

with glass cloth buffer to prevent tearing of the vacuum bag over the sharp corners of this plate.

Curing was accomplished in a blanket press autoclave. The autoclave was preheated to a temperature of 322°K (120°F). Vacuum bagging was accomplished by means of a neoprene blanket covering the layup and clamped between the two platens of the press. Initially, vacuum was applied for 25 minutes to facilitate wetting of the fibers before application of the separator and bleeder cloths. The specimen was removed from the autoclave temporarily, for the addition of two bleeder layers. In the first stage of curing, the specimen was subjected to full vacuum and a pressure of 276 kPa (40 psi) for 25 minutes at a temperature of 322°K (120°F). The partially cured plate was then removed from the autoclave and placed in the freezer for 5 minutes. When the resin became firm enough, the separator and glass bleeder layers were removed and replaced with a 0.051 mm (0.002 in.) thick teflon film. The plate was then post-cured for one hour under 690 kPa (100 psi) pressure at a temperature of 342°K (155°F).

The procedure described above was used to fabricate ten $[+45_4/-45_4]_{2s}$ and ten $[0_4/+45_4/-45_4/90_4]_s$ plates 33 cm x 33 cm (13 in. x 13 in.). The nominal thickness was 0.203 cm (0.080 in.). (These plates were designated as 300 and 400 series, respectively.)

4.3 LAMINATES WITH EMBEDDED FLAWS

A new laminate fabrication process was developed for this phase of the program. Type 1062 glass roving obtained from PPG Industries was used. This roving was dry-wound over various metal frames to produce windings for the various laminates. Unidirectional plates were started by winding the glass roving over an open steel frame of dimensions 35.6 cm x 44.5 cm (14 in. x 17.5 in.) in a filament winding machine (Figure 20). Four complete windings were used for an eight-ply plate. In this new fabrication process the ply thickness was approximately four times the ply thickness obtained by the process described before. The glass roving was taped along the two edges normal to the fiber direction after every winding to prevent slippage of the glass during winding of additional plies. The frame had screw adjustments to allow a slight translation of one of the bars over which the glass is wound. This adjustment

is made after completion of the winding to release some of the tension in the roving. Some slack is necessary because of the finite width of the frame (0.64 cm; 0.25 in.) to allow all plies to come together.

Angle-ply $[+45_2/-45_2]_s$ laminates were started by winding glass roving over a larger steel frame of dimensions 59.1 cm x 59.1 cm (23.25 in. x 23.25 in.). Two complete windings in two perpendicular directions were used. The large frame used allows a minimum 35.6 cm x 35.6 cm (14 in. x 14 in.) square to be cut from the center with the sides at 45-deg to the fibers.

Fiber winding for quasi-isotropic laminates was a little more complicated. First, the 90-deg plies are wound over a small steel frame of inside dimensions 35.6 cm x 35.6 cm (14 in. x 14 in.). One complete winding is used for the two center 90-deg plies. This frame is then mounted inside a large square frame having sides at 45-deg with the fibers, and the 45-deg plies are wound over two sides of the large frame (Figure 21). After completion of the 45-deg winding, the large frame was turned and mounted across the other sides and the -45-deg plies were wound (Figure 22). After completion of this winding, two pairs of bars with screws were mounted on the two sides of the frame at 45-deg with the sides and parallel to the 90-deg fibers in the interior. The screws were spaced 1.02 cm (0.4 in.) apart to correspond to twice the spacing of the roving during winding. The final outer 0-deg plies were layed by threading the glass roving by hand around the screw posts using a specially made threader (Figure 23).

Flaws in the form of film patches simulating delaminations were embedded between the various plies of the winding. Two types of flaws were used, teflon patches 0.076 mm (0.003 in.) thick and Kapton (polyimide) film pillows. The latter were made by heat sealing or bonding two 0.025 mm (0.001 in.) thick Kapton films along the periphery of the flaw patch leaving the area around the center unbonded. This is considered an acceptable means for simulating delaminations. The inclusions were of two shapes, square and round and of two sizes, 1.27 cm (0.50 in.) and 0.64 cm (0.25 in.) side or diameter.

Eighteen inclusions were embedded in each laminate as shown in Figure 24. They were at least 6.35 cm (2.5 in.) apart, arranged in three rows as shown. They were embedded between the second and third ply and between the fourth and fifth ply (middle surface). The inclusions were inserted in the intended locations in the dry winding by means of tweezers.

A quantity of 150 g of the Maraset 658/558 system was mixed as before. Half of this quantity was poured on one side of the winding and spread over the central area as uniformly as possible. Then, the wet layup was covered with a 0.051 mm (0.002 in.) thick teflon sheet (Figure 25). The plate was turned over, the remaining half of the resin was poured over it and spread and the plate was covered with another similar teflon sheet.

The frame with the wet layup between teflon sheets was mounted over a 1.91 cm (0.75 in.) thick plywood plate with a 35 cm x 35 cm (13.75 in. x 13.75 in.) square cutout. The assembly was placed in the autoclave press over a 1.91 cm (0.75 in.) thick 33 cm x 33 cm (13 in. x 13 in.) steel plate. A second steel pressure plate was placed on top of the layup (Figure 26). This plate was blocked with wooden liners to blunt the sharp edges. Finally, the assembly was covered with glass cloth to provide vacuum passage and the rubber blanket (Figure 27). Full vacuum was drawn and a pressure of 656 kPa (95 psi) applied. The vacuum was cut off after 30 minutes and the plate cured under pressure at room temperature in approximately 18 hours.

Six plates with embedded flaws were fabricated, two of each of the $[0_8]$, $[\pm 45]_{2s}$, and $[0/\pm 45/90]_s$ layups. The nominal thickness was 0.216 cm (0.085 in.). Photographs of typical plates are shown in Figures 28, 29, and 30.

4.4 THICK LAMINATES

The same procedures used in fabrication of laminates with embedded flaws were used to fabricate thick laminates. Sixteen-ply laminates of the following layups were fabricated: $[0]_{16}$, $[+45_2/-45_2]_{2s}$ and $[0_2/+45_2/-45_2/90_2]_s$. The glass roving was wound around the frames as before, but with twice as many windings in each direction. Twice as much resin (300 g) was used to wet a 33 cm x 33 cm (13 in. x 13 in.) area in the center of the winding. The plates were cured at room temperature under pressure and vacuum as discussed before. Nine plates were fabricated, three of each of the three layups mentioned above. The ply thickness was the same as in the case of plates with inclusions and approximately four times the ply thickness obtained by using Style 3733 glass cloth as discussed before. The nominal thickness of the thick laminates was 0.427 cm (0.168 in.).

5. MECHANICAL AND OPTICAL CHARACTERIZATION

5.1 MATRIX RESIN

The matrix material was the Maraset 658/558 system obtained by mixing Maraset 658 epoxy resin with Maraset 558 hardener in a 2:1 ratio.

The density of the resin determined by measuring the volume and weight of a small prismatic sample is:

$$\rho_m = 1,185 \text{ kg/m}^3 (0.043 \text{ lb/in.}^3)$$

Mechanical and optical properties were determined by testing under uniaxial tension, a coupon specimen 20.3 cm (8 in.) long, 2.54 cm (1.00 in. wide) and 0.241 cm (0.095 in.) thick instrumented with strain gages. Stress-strain curves are shown in Figure 31. The stress-birefringence curve is shown in Figure 32. Properties obtained from these curves are:

$$E = 3.39 \text{ GPa } (0.49 \times 10^6 \text{ psi})$$

$$\nu = 0.36$$

$$f = 9.29 \frac{\text{kPa-m}}{\text{fr}} (53.0 \frac{\text{psi-in.}}{\text{fr}})$$

5.2 UNIDIRECTIONAL GLASS/EPOXY (MARASET/3733)

The material used in the first batch of composite plates made of Maraset 658/558 resin and Style 3733 glass was characterized by testing coupons cut from a unidirectional $[0_{30}]$ composite plate.

The density determined by weighing a prismatic sample and measuring its volume is:

$$\rho_c = 1,926 \text{ kg/m}^3 (0.070 \text{ lb/in.}^3)$$

The fiber volume ratio, V_f , was determined by the gravimetric method using the following relation:

$$V_f = \frac{\rho_c - \rho_m}{\rho_f - \rho_m} \quad (12)$$

where

ρ_c , ρ_m , and ρ_f = densities of composite, matrix, and fiber, respectively.

Using the measured values of composite and matrix densities and the known value of $\rho_f = 2,540 \text{ kg/m}^3$ for the glass fibers, we obtain

$$V_f = 0.547$$

The values above are based on a sample thickness of 2.11 mm (0.083 in.).

Coupons were machined from one of the $[0_{30}]$ laminates made with Style 3733 glass at 0-, 90-, and 45-deg to the fiber direction for mechanical and optical characterization. These coupons were 2.54 cm (1.0 in.) wide, 22.9 cm (9 in.) long and 2.16 to 2.26 mm (0.085 to 0.089 in.) thick. They were instrumented with strain gages and loaded in tension in the polariscope. Birefringence and strain measurements were taken at each of several load levels. Stress-strain and stress-birefringence curves for the 0-, 90-, and 45-deg specimens are shown in Figures 33 to 38. Mechanical properties obtained from these curves are:

$$E_{11} = 38.2 \text{ GPa } (5.54 \times 10^6 \text{ psi})$$

$$E_{22} = 11.5 \text{ GPa } (1.67 \times 10^6 \text{ psi})$$

$$E_{45} = 10.6 \text{ GPa } (1.54 \times 10^6 \text{ psi})$$

$$\nu_{12} = 0.30$$

$$\nu_{21} = 0.08$$

$$(\nu_{xy})_{\theta=45^\circ} = 0.40$$

The ratio of the longitudinal to the transverse modulus is 3.32.

Photoelastic properties obtained from the stress-birefringence curves are:

$$f_{11} = 73.0 \frac{\text{kPa-m}}{\text{fr}} (417 \frac{\text{psi-in.}}{\text{fr}})$$

$$f_{22} = 40.1 \frac{\text{kPa-m}}{\text{fr}} (229 \frac{\text{psi-in.}}{\text{fr}})$$

$$f_{45} = 34.9 \frac{\text{kPa-m}}{\text{fr}} (199 \frac{\text{psi-in.}}{\text{fr}})$$

Substituting the values above in Equation 5, we obtain:

$$f_{12} = 71.1 \frac{\text{kPa-m}}{\text{fr}} (406 \frac{\text{psi-in.}}{\text{fr}})$$

The $[0_{30}]$ glass/epoxy specimen was tested again in tension to determine the mechanical and birefringent behavior of the material to failure. Stress-strain and stress-birefringence curves are shown in Figure 39. The axial strain remains linear up to a value of 0.010 corresponding to a stress of 386 MPa (56 ksi). Thereafter, it becomes nonlinear increasing at a slightly higher rate to failure. The strength and ultimate strain were:

$$S_{11T} = 607 \text{ MPa (88 ksi)}$$

$$\epsilon_{11T}^u = 0.0161$$

The birefringence response remains linear up to at least a fringe order of 4, corresponding to a uniaxial tensile stress of 310 MPa (45 ksi). Beyond this point the birefringence of the material becomes indistinct and fringe orders cannot be resolved. The limitation in fringe resolution is related to the inhomogeneity of the composite material and the slight mismatch in index of refraction between the resin matrix and glass fibers. This limitation is more pronounced with increasing fiber volume ratio.

The measured mechanical and optical properties were compared with analytical predictions. The longitudinal modulus predicted by the rule of mixtures is given by

$$E_{11} = V_f E_f + (1 - V_f) E_m \quad (13)$$

where

V_f = fiber volume ratio

E_f, E_m = fiber and matrix moduli, respectively.

Substituting the values:

$$V_f = 0.547$$

$$E_f = 72.5 \text{ GPa } (10.5 \times 10^6 \text{ psi})$$

$$E_m = 3.39 \text{ GPa } (0.49 \times 10^6 \text{ psi})$$

we obtain

$$E_{11} = 41.1 \text{ GPa } (5.96 \times 10^6 \text{ psi})$$

which is higher than the measured value of 38.2 GPa (5.54×10^6 psi). The agreement is a much better one if the fiber volume ratio of the sample is adjusted for the larger specimen thickness than that on which the value of V_f is based. Thus, the adjusted density of the tensile specimen is:

$$\rho_c = 1,926 \frac{t_0}{t} = 1,926 \left(\frac{83}{87}\right) = 1,837 \text{ kg/m}^3$$

where t_0 and t are the thickness of the reference and test specimens, respectively. The adjusted fiber volume ratio then is $V_f = 0.482$. Using this value in the rule of mixture we obtain a predicted value for the modulus

$$E_{11} = 36.6 \text{ GPa } (5.31 \times 10^6 \text{ psi})$$

The fringe values determined experimentally were compared with those predicted by the stress-proportioning concept proposed by Dally and Prabhakaran.¹² The longitudinal fringe value is predicted by the relation

$$f_{11} = f_L = \frac{[V_f + (E_m/E_f) V_m] f_f f_m}{V_f f_m + V_m f_f (E_m/E_f)} \quad (14)$$

where

f_f, f_m = fiber and matrix fringe values

V_m = matrix volume ratio.

Substituting the values:

$$V_f = 0.482$$

$$V_m = 0.518$$

$$E_m = 3.39 \text{ GPa } (0.49 \times 10^6 \text{ psi})$$

$$E_f = 72.5 \text{ GPa } (10.5 \times 10^6 \text{ psi})$$

$$f_m = 9.29 \frac{\text{kPa-m}}{\text{fr}} (53.0 \frac{\text{psi-in.}}{\text{fr}})$$

$$f_f = 119.1 \frac{\text{kPa-m}}{\text{fr}} (680 \frac{\text{psi-in.}}{\text{fr}}) \text{ (Reference 12)}$$

we obtain

$$f_{11} = 76.0 \frac{\text{kPa-m}}{\text{fr}} (434 \frac{\text{psi-in.}}{\text{fr}})$$

which is in very good agreement with the measured value.

The transverse fringe value is predicted by the relation:¹²

$$f_{22} = f_T = \frac{\left[V_f^* + V_m^* \frac{E_m^*}{E_f^*} \frac{1 + \nu_f}{1 + \nu_m} \right] f_f f_m}{V_f f_m + V_m f_f \frac{E_m^*}{E_f^*} \frac{1 + \nu_f}{1 + \nu_m}} \quad (15)$$

where

ν_f, ν_m = Poisson's ratios of fiber and matrix materials, respectively

$$V_f^* = \sqrt{V_f / \pi}$$

$$V_m^* = 1 - V_f^*$$

$$E_m^* = E_m / (1 - \nu_m^2)$$

$$E_f^* = \frac{E_m^* + 2V_f (E_f - E_m^*)}{1 + [2V_f^* (1 - 2V_f^*) / E_m^* E_f] [(E_f - E_m^*)^2 - (\nu_m E_f - \nu_f E_m^*)^2]}$$

Substituting the various measured and computed values of constants and parameters, including the value of $\nu_f = 0.2$,¹² we obtain:

$$f_{22} = f_T = 33.5 \frac{\text{kPa-m}}{\text{fr}} (191 \frac{\text{psi-in.}}{\text{fr}})$$

which is somewhat lower than the measured value of 229 (psi-in.)/fringe.

The shear fringe value is predicted by the relation:¹²

$$f_{12} = \frac{2 \left[\nu_f^* + (G_m^*/G_f^*) \nu_m^* \right] f_f f_m}{\nu_f f_m + \nu_m f_f (G_m^*/G_f^*)} \quad (16)$$

where

$$G_m^* = G_m / [1 - 2\nu_m^2 / (1 - \nu_m)]$$

$$G_f^* = G_m G_f / [G_f + 2\nu_f^* (G_m^* - G_f)]$$

G_f, G_m = shear modulus of fiber and matrix materials, respectively.

Substituting measured and computed values in Equation 16 we obtain:

$$f_{12} = 58.2 \frac{\text{kPa-m}}{\text{fr}} (332 \frac{\text{psi-in.}}{\text{fr}})$$

which is lower than the value of 71.1 $\frac{\text{kPa-m}}{\text{fr}}$ (406 $\frac{\text{psi-in.}}{\text{fr}}$) computed from measured quantities.

Experimental results for birefringent properties were also compared with predictions obtained by Knight and Pih using a finite element analysis.¹⁸ The predicted properties are:

$$f_{11} = 70.1 \frac{\text{kPa-m}}{\text{fr}} (400 \frac{\text{psi-in.}}{\text{fr}})$$

$$f_{22} = 39.0 \frac{\text{kPa-m}}{\text{fr}} (223 \frac{\text{psi-in.}}{\text{fr}})$$

$$f_{12} = 47.3 \frac{\text{kPa-m}}{\text{fr}} (270 \frac{\text{psi-in.}}{\text{fr}})$$

Of these values, the longitudinal and transverse fringe values are in good agreement with measured quantities, but the shear fringe value is much lower than the one computed from measured properties.

5.3 UNIDIRECTIONAL GLASS/EPOXY (MARASET/1062)

This material which was used for the laminates with flaws and the thick laminates was fabricated using glass roving in the filament winding process described previously. It is expected that birefringent and mechanical properties of this material may be somewhat different from those of the material with Style 3733 glass. However, the characterization of this additional batch of material was not completed because of time and fund limitations.

6. SUMMARY, CONCLUSIONS, AND RECOMMENDATIONS FOR FUTURE WORK

Materials were selected and fabrication procedures developed for orthotropic birefringent materials. The Maraset 658/558 system consisting of Maraset 658 epoxy and Maraset 558 hardener was selected as the matrix resin. This resin has a pot life of several hours and cures at room temperature with a minimum amount of shrinkage, producing a water-clear casting. In the first batch of composite plates fabricated, the reinforcing fibers were obtained from Style 3733 glass cloth (J. P. Stevens and Co.) with S-910 finish. In the second batch of plates fabricated Type 1062 glass roving (PPG Industries) was used.

Two different fabrication procedures were used. In the first one, layers of unidirectional fibers were obtained by removing the fill fibers from the glass cloth, stacked and impregnated with the resin matrix. The wet layup was bagged with bleeder cloths and cured in an autoclave at an elevated temperature of 342°K (155°F). Ten plates of each of the $[0_{30}]$, $[+45_4/-45_4]_{2S}$, and $[0_4/+45_4/-45_4/90_4]_S$ layups were fabricated.

In the second fabrication procedure, the glass roving was dry-wound over various metal frames to produce windings for the various laminates. The dry windings were impregnated with resin and the layups were cured at room temperature under pressure and vacuum in a blanket press autoclave. Six plates, two of each of the $[0_8]$, $[\pm 45]_{2S}$, and $[0/\pm 45/90]_S$ layups, were fabricated with embedded teflon and Kapton disks. An additional nine plates were fabricated, three of each of the $[0_{16}]$, $[+45_2/-45_2]_{2S}$, and $[0_2/+45_2/-45_2/90_2]_S$ layups.

The matrix and the unidirectional glass/epoxy material were fully characterized. The density, fiber volume ratio, mechanical, and optical properties were determined. Results for the latter were in good agreement with predictions based on a stress-proportioning concept and also, with one exception, with properties predicted by a finite element analysis.

The last fabrication procedure developed is more advantageous as it can be used to produce laminates of any desired layup at least up to sixteen plies thick. Thickness control to within small tolerances of ± 0.102 mm (± 0.004 in.) is still difficult. Some further refinements are needed to insure better uniformity among plates, since it was shown that the fiber volume ratio is very sensitive to the laminate thickness.

The birefringence response of the material developed should be studied further as a function of fiber volume ratio, off-axis fiber orientation, and layup in multi-directional laminates. In the latter case, the predictive ability of various theories should be checked with direct experimental measurements of both birefringence and isoclinic parameters.

The availability of transparent composite laminates of various layups affords the possibility of conducting macromechanical stress analyses by means of anisotropic photoelasticity. Stress distributions around stress raisers such as holes, cracks, and other defects can be studied experimentally. Thickness effects can be studied using the thicker laminates fabricated in this program.

The property of transparency and birefringence should be utilized in studying failure modes in notched and unnotched laminates, failure initiation, and failure propagation. The use of stereoscopic photography should be investigated as a means of determining the location of flaws and failures through the thickness. The study of failure initiation in the form of microcracks between fibers in various plies during cyclic fatigue is of great importance and could be greatly facilitated with these transparent composites.

The ability to see and locate flaws easily should help in studying their influence and failure growth around them during service loading. Furthermore, the ability to detect and characterize flaws optically should serve to set standards for calibration of conventional nondestructive evaluation instrumentation such as ultrasonics.

The method of anisotropic photoelasticity should be further utilized in structural applications of composites, such as bonded or bolted joints.

REFERENCES

1. I.M. Daniel and A.J. Durelli, "Photoelastic Investigation of Residual Stresses in Glass-Plastic Composites," Proc. of 16th Conf. of Reinf. Plastics Div., Soc. of Plastics Industry, Sect. 19-A, February 1961.
2. R.H. Marloff and I.M. Daniel, "Three-Dimensional Photoelastic Analysis of a Fiber-Reinforced Composite Model," Experimental Mechanics, Vol 9, pp. 156-162, April 1969.
3. D.M. Schuster and E. Scala, "The Mechanical Interaction of Sapphire Whiskers with a Birefringent Matrix," Trans. of Metall. Soc. AIME, Vol. 230, p. 1635, 1964.
4. I.M. Daniel, "Micromechanics" in "Structural Airframe Application of Advanced Composite Materials," AFML-TR-69-101, Vol. II, September 1969.
5. J.W. Dally and I. Alfievich, "Application of Birefringent Coatings to Glass-Fiber-Reinforced Plastics," Experimental Mechanics, Vol. 9, pp. 97-102, 1969.
6. I.M. Daniel, R.E. Rowlands and J.B. Whiteside, "Deformation and Failure of Boron-Epoxy Plate with Circular Hole," Analysis of the Test Methods for High Modulus Fibers and Composites, ASTM STP 521, American Society for Testing and Materials, pp. 143-164, 1973.
7. I.M. Daniel, R.E. Rowlands and J.B. Whiteside, "Effects of Material and Stacking Sequence on Behavior of Composite Plates with Holes," Experimental Mechanics, Vol. 14, pp. 1-9, January 1974.
8. I.M. Daniel, "Strain and Failure Analysis in Graphite/Epoxy Plates with Cracks," Experimental Mechanics, Vol. 18, July 1978.
9. G.A. Horridge, "A Polarized Light Study of Glass Fibre Laminates," British J. of Appl. Physics, Vol. 6, p. 314, 1955.
10. H. Pih and C.E. Knight, "Photoelastic Analysis of Anisotropic Fiber Reinforced Composites," J. Composite Materials, Vol. 3, pp. 94-107, January 1969.
11. R.C. Sampson, "A Stress-Optic Law for Photoelastic Analysis of Orthotropic Composites," Experimental Mechanics, Vol. 10, No. 5, pp. 210-215, May 1970.
12. J.W. Dally and R. Prabhakaran, "Photo-Orthotropic Elasticity," Experimental Mechanics, Vol. 11, No. 8, pp. 346-356, August 1971.
13. C.W. Bert, "Theory of Photoelasticity of Birefringent Filamentary Composites," Fibre Science and Technology, Vol. 5, pp. 165-171, 1972.

14. R.B. Pipes and J.L. Rose, "Strain-Optic Law for a Certain Class of Birefringent Composites," Experimental Mechanics, Vol. 14, No. 9, pp. 355-360, September 1974.
15. R. Prabhakaran, "On the Stress-Optic Law for Orthotropic Model Materials in Biaxial Stress Fields," Experimental Mechanics, Vol. 15, pp. 29-34, January 1975.
16. R. Prabhakaran, "A Strain-Optic Law for Orthotropic Model Materials," AIAA Journal, Vol. 13, pp. 723-728, 1975.
17. J. Cernosek, "Note on Photoelastic Response of Composites," Experimental Mechanics, Vol. 15, pp. 354-357, September 1975.
18. C.E. Knight and H. Pih, "Orthotropic Stress-Optic Law for Plane Stress Photoelasticity of Composite Materials," Fibre Science and Technology, Vol. 9, pp. 297-313, 1976.
19. R. Prabhakaran and J.W. Dally, "The Application of Photo-Orthotropic Elasticity," J. Strain Analysis, Vol. 7, No. 4, pp. 253-260, 1972.
20. I.M. Daniel, "Photoelastic Studies of Mechanics of Composites," Progress in Experimental Mechanics - Durelli Anniversary Volume, The Catholic University of America, 1975.
21. B.D. Agarwal and S.K. Chaturvedi, "Improved Birefringent Composites and Assessment of Photoelastic Theories," Fibre Science and Technology, Vol. 11, No. 6, pp. 399-412, 1978.
22. J.E. Ashton, J.C. Halpin and P.H. Petit, Primer on Composite Materials: Analysis, Technomic Publishing Co., Stamford, Connecticut, p. 17, 1969.

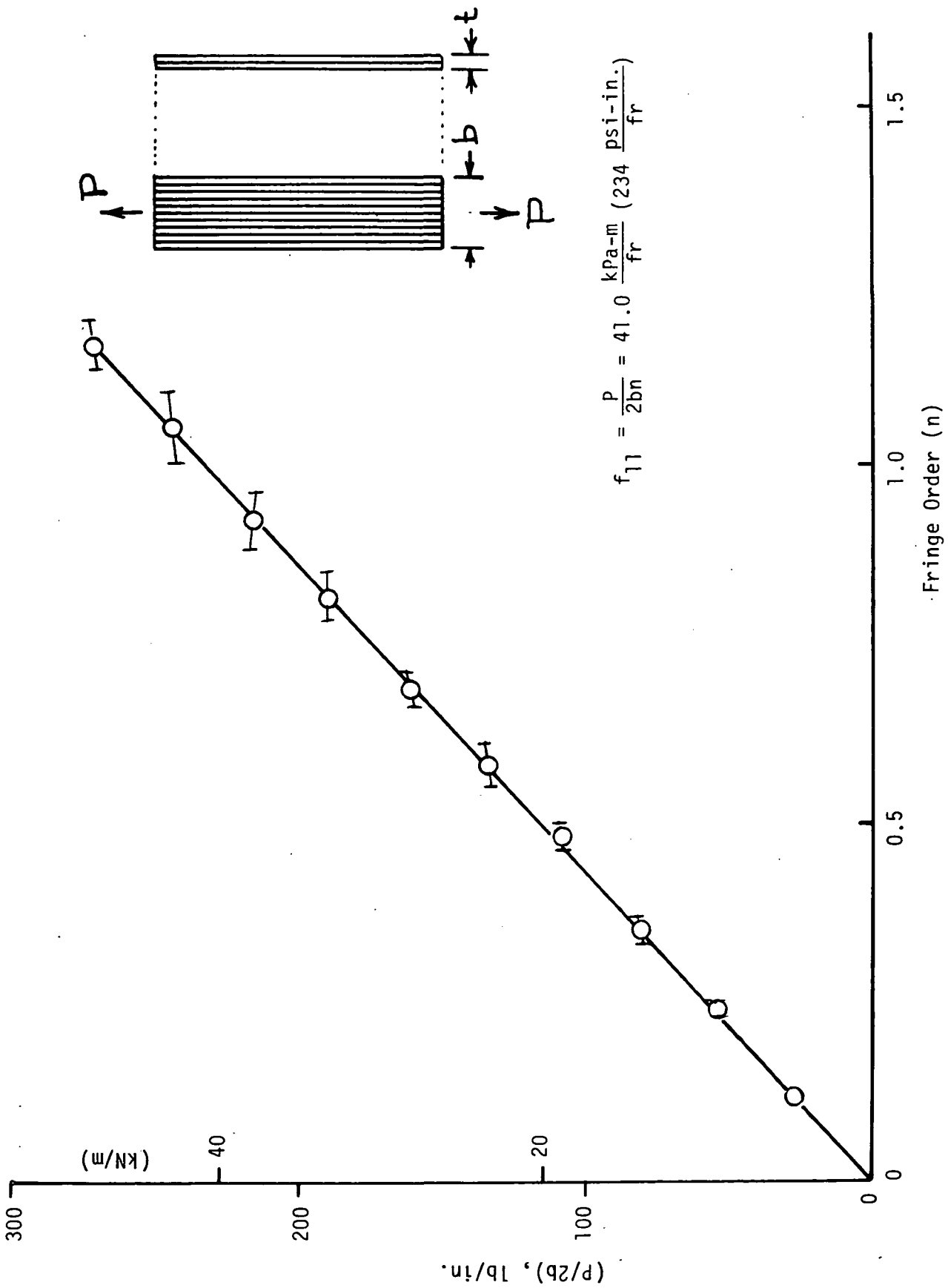


Figure 1. Load-birefringence curve for $[0_{15}]$ glass/Maraset composite under uniaxial tensile loading.
(Style 7500; Specimens 1 and 2)

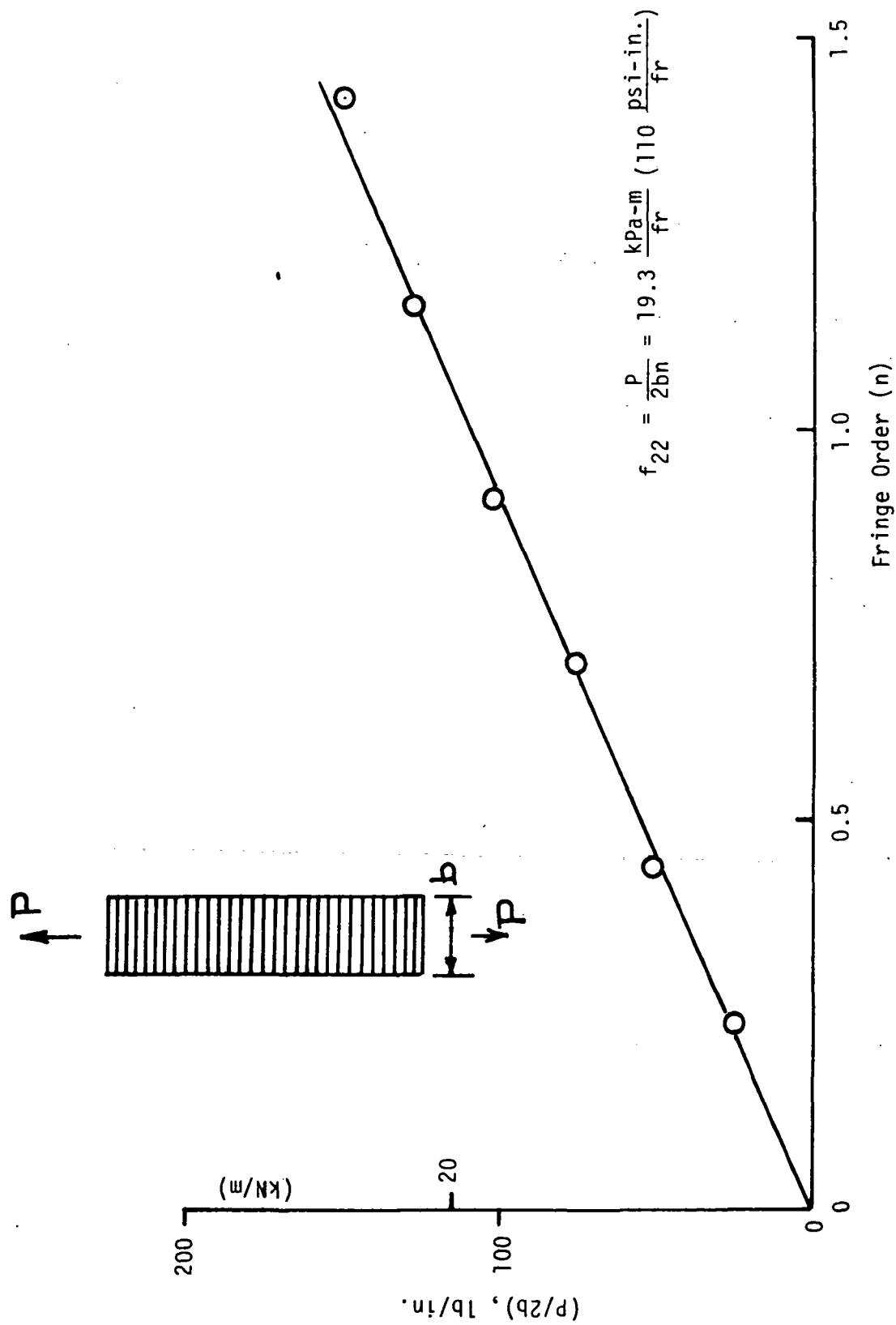


Figure 2. Load-birefringence curve for $[90_{15}]$ glass/Maraset composite under uniaxial tensile loading.
(Style 7500; Specimens 3 and 4)

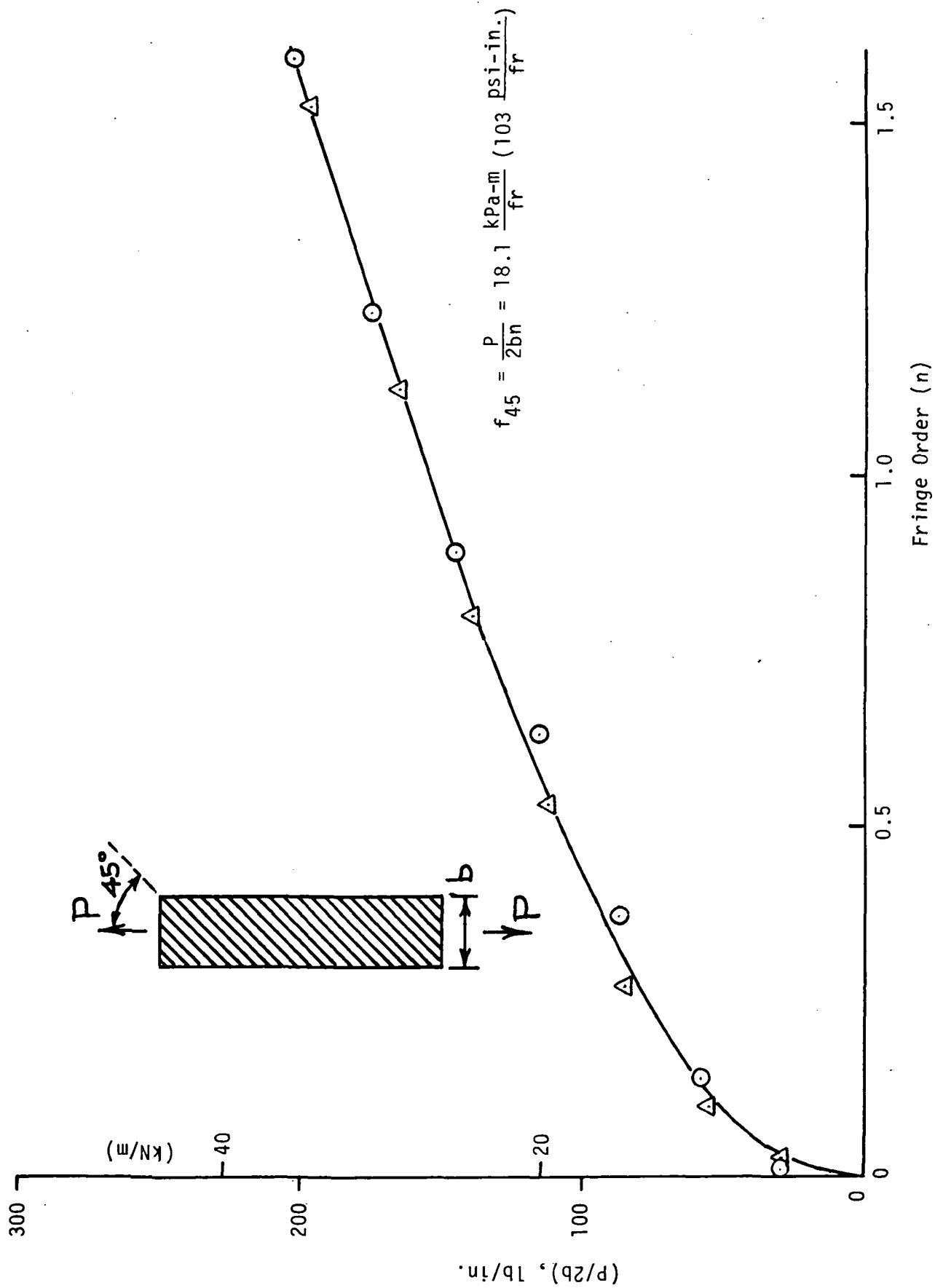


Figure 3. Load-birefringence curve for $[45_{15}]$ glass/Maraset composite under uniaxial tensile loading.
(Style 7500; Specimens 5 and 6)

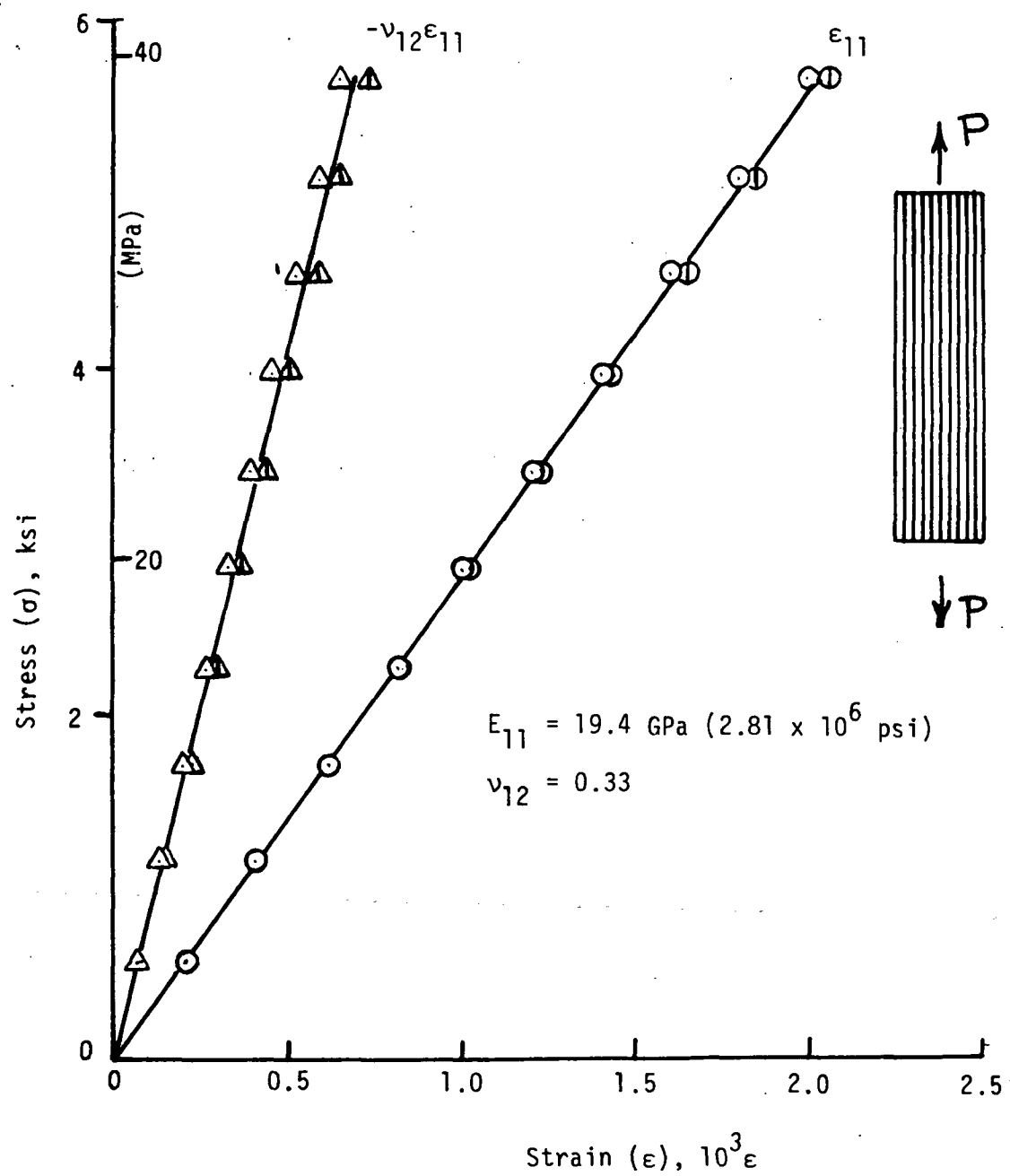


Figure 4. Stress-strain curves for $[0_{15}]$ glass/Maraset Composite under uniaxial tensile loading (Style 7500; Specimens 1 and 2).

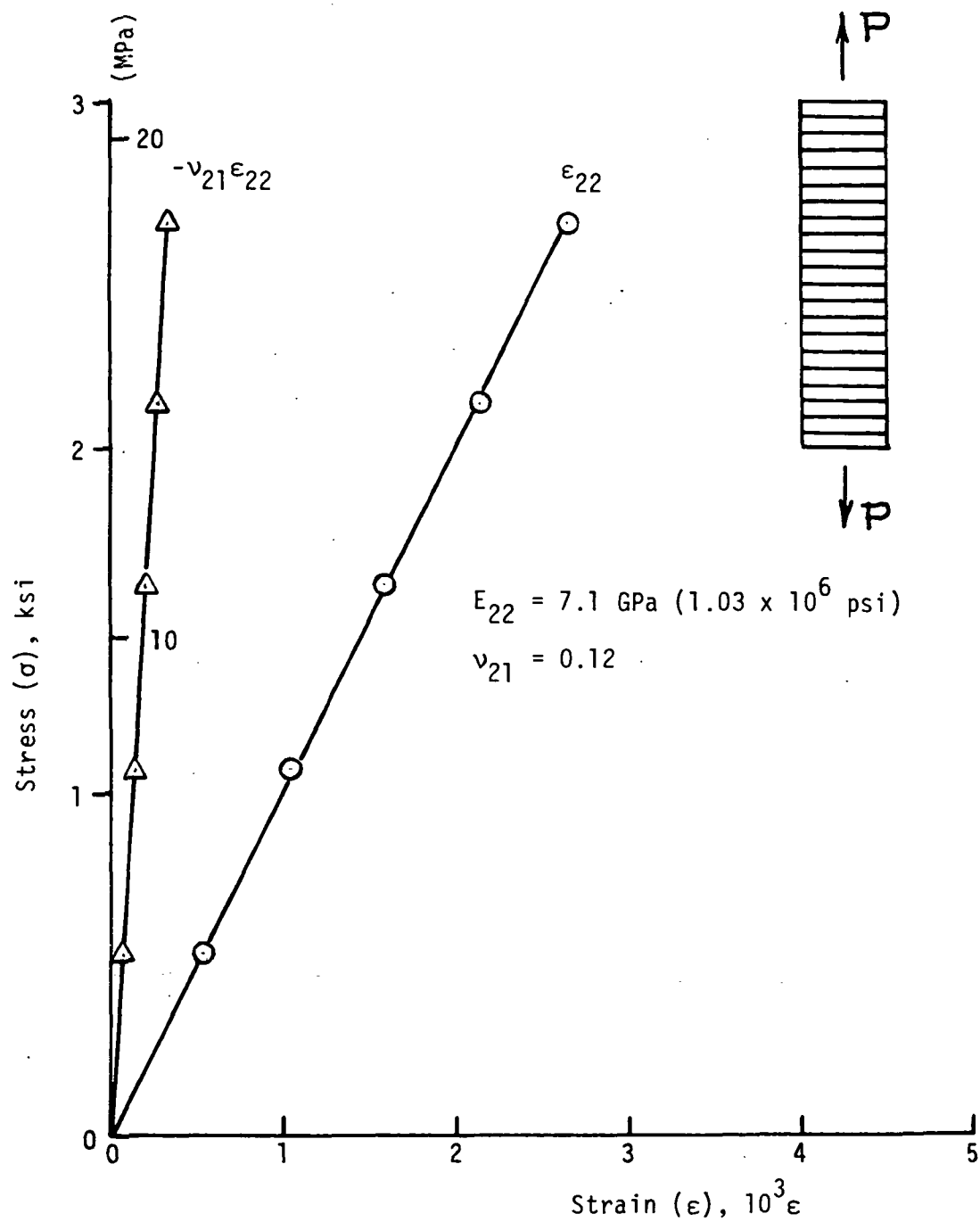


Figure 5. Stress-strain curves for $[90_{15}]$ glass/Maraset Composite under uniaxial tensile loading (Style 7500; Specimen 4).

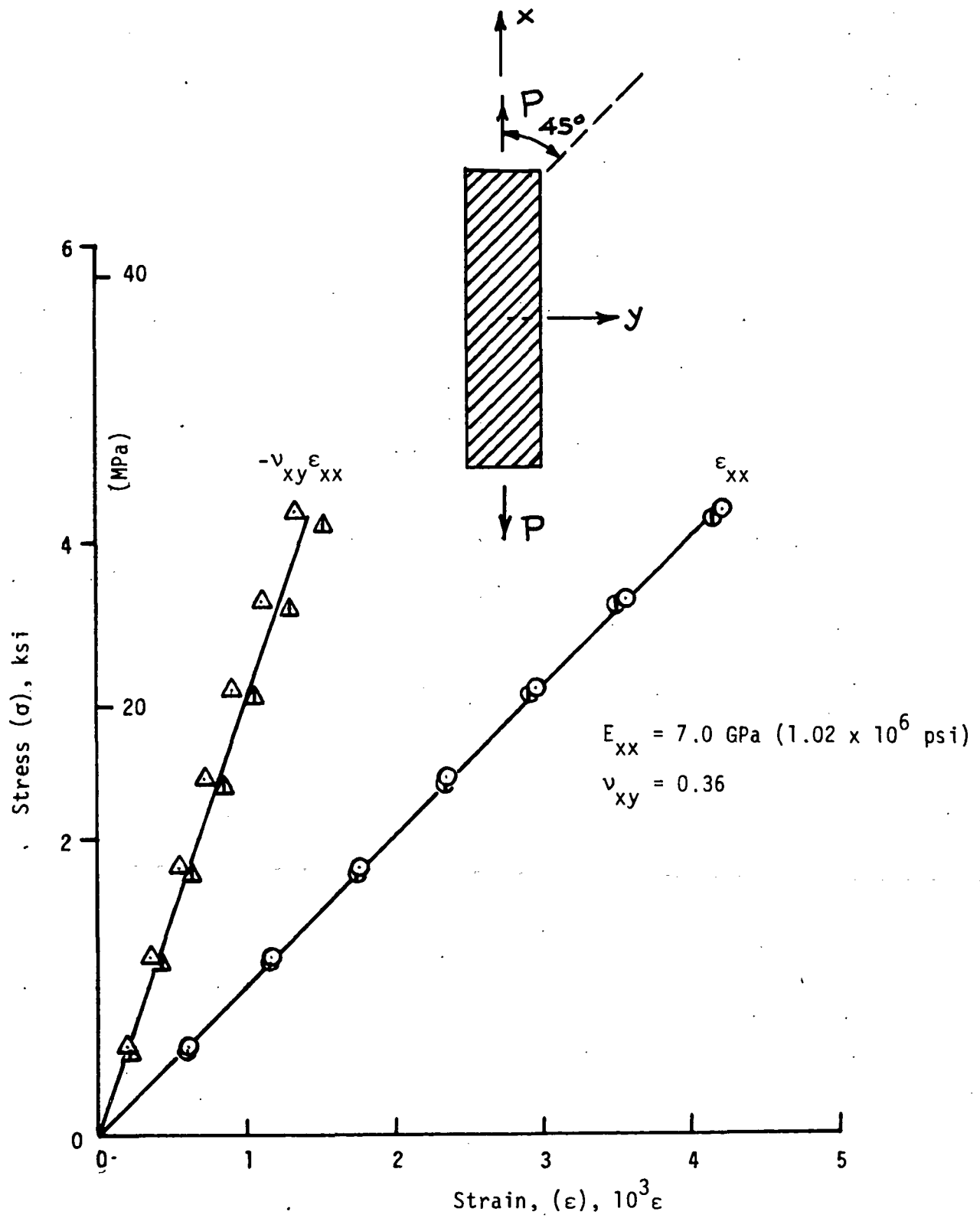


Figure 6. Stress-strain curves for $[45]_5$ glass/Maraset composite under uniaxial tensile loading (Style 7500; Specimens 5 and 6).

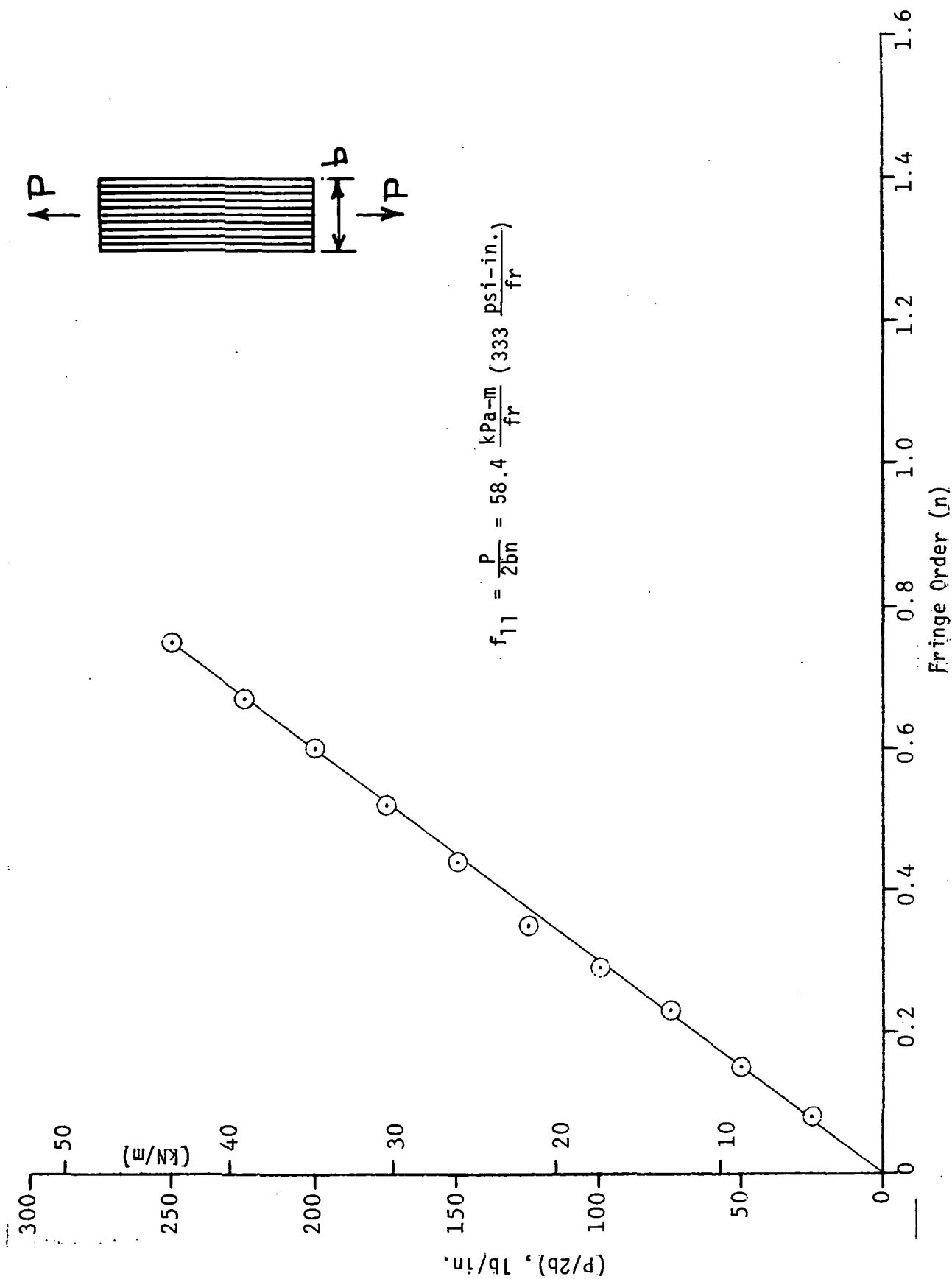


Figure 7. Load-birefringence curve for [030] glass/Maraset composite under uniaxial tensile loading (Style 3733; Specimen No. 42-1).

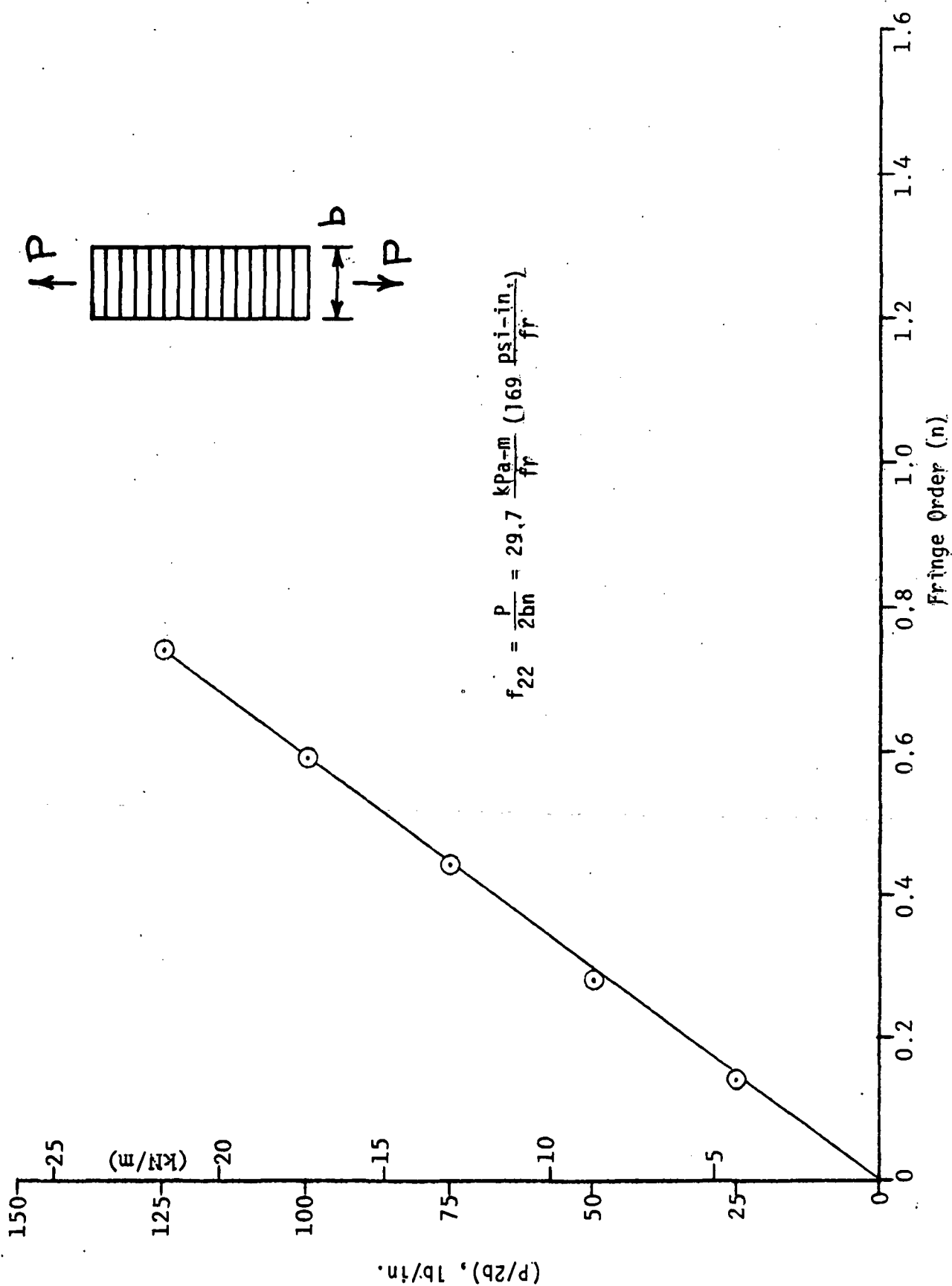


Figure 8. Load-birefringence curve for $[90_{30}]$ glass/Maraset composite under uniaxial tensile loading (Style 3733; Specimen No. 42-2).

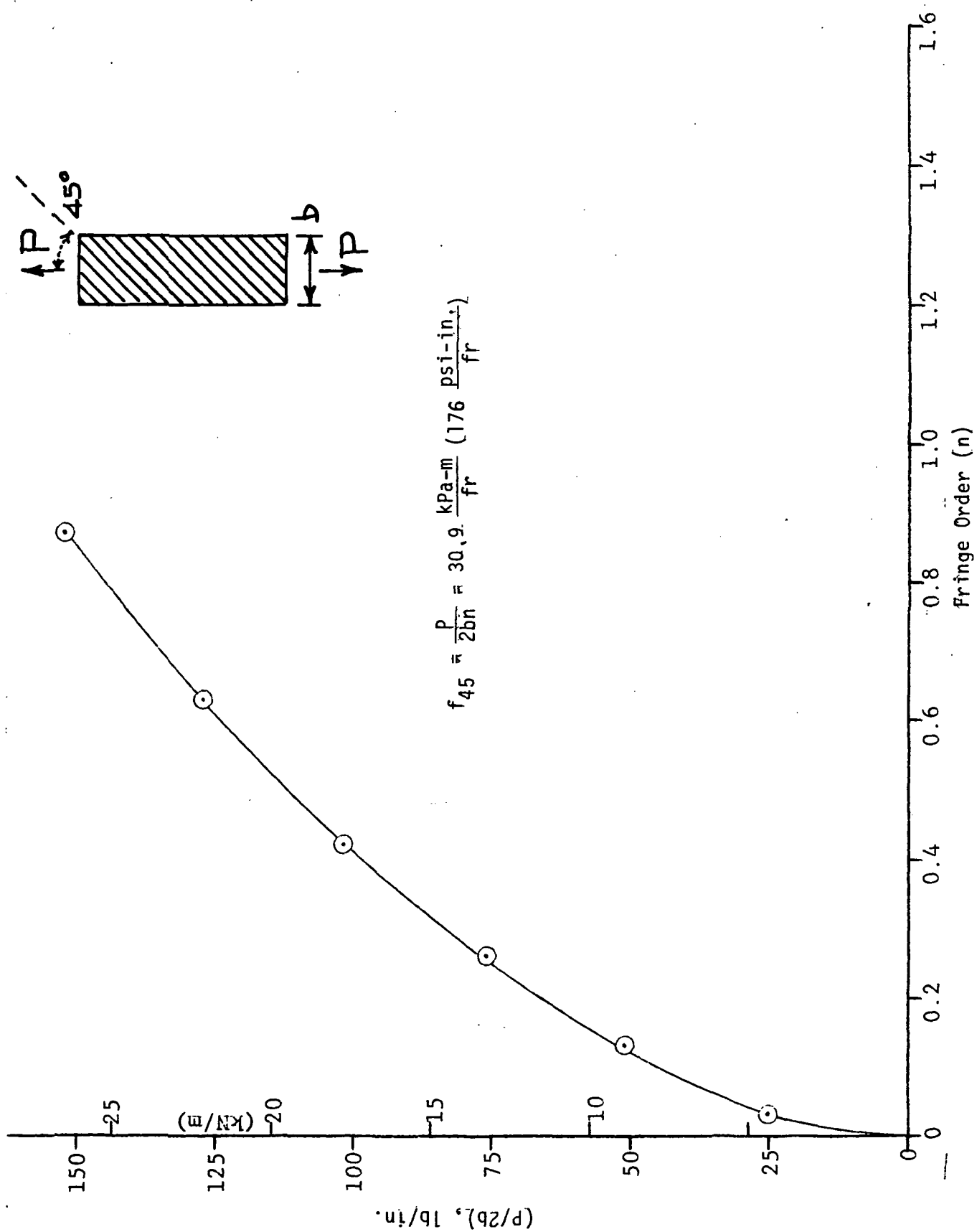


Figure 9. Load-birefringence curve for [45/30] glass/Maraset composite under uniaxial tensile loading (Style 3733; Specimen No. 42-3).

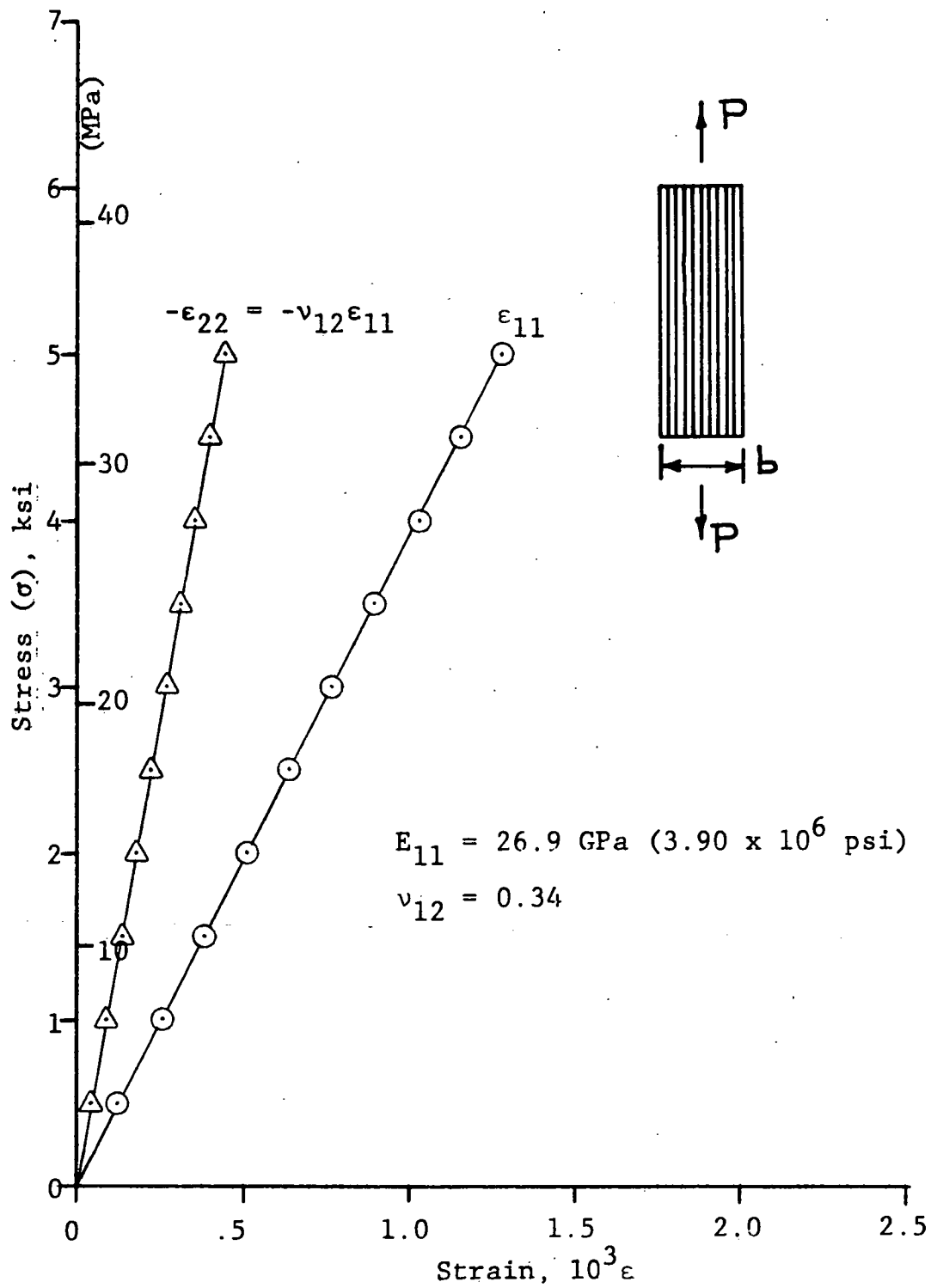


Figure 10. Stress-strain curves for $[0_{30}]$ glass/Maraset composite under uniaxial tensile loading (Style 3733; Specimen No. 42-1).

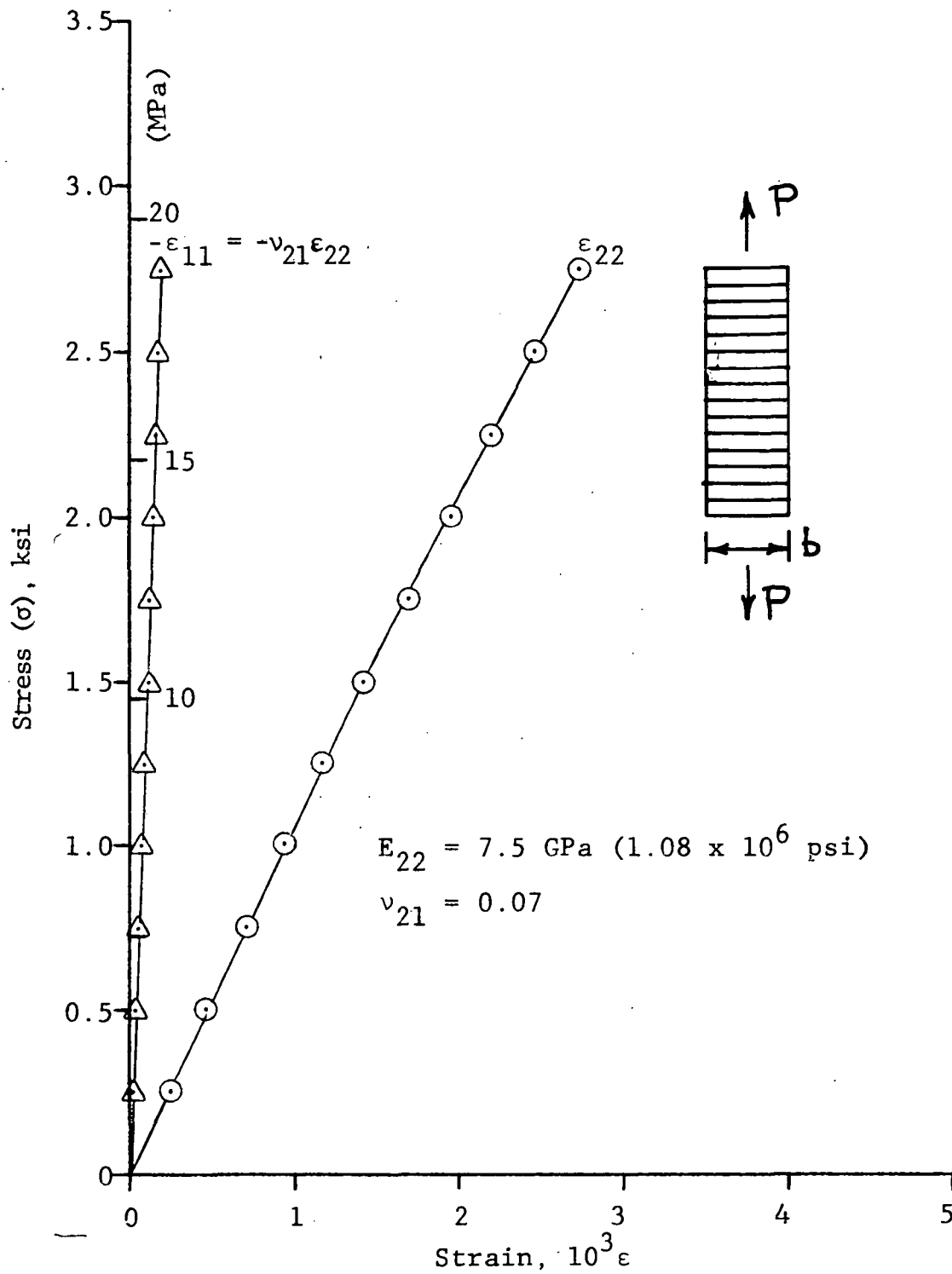


Figure 11. Stress-strain curves for $[90_{30}]$ glass/Maraset composite under uniaxial tensile loading (Style 3733; Specimen No. 42-2).

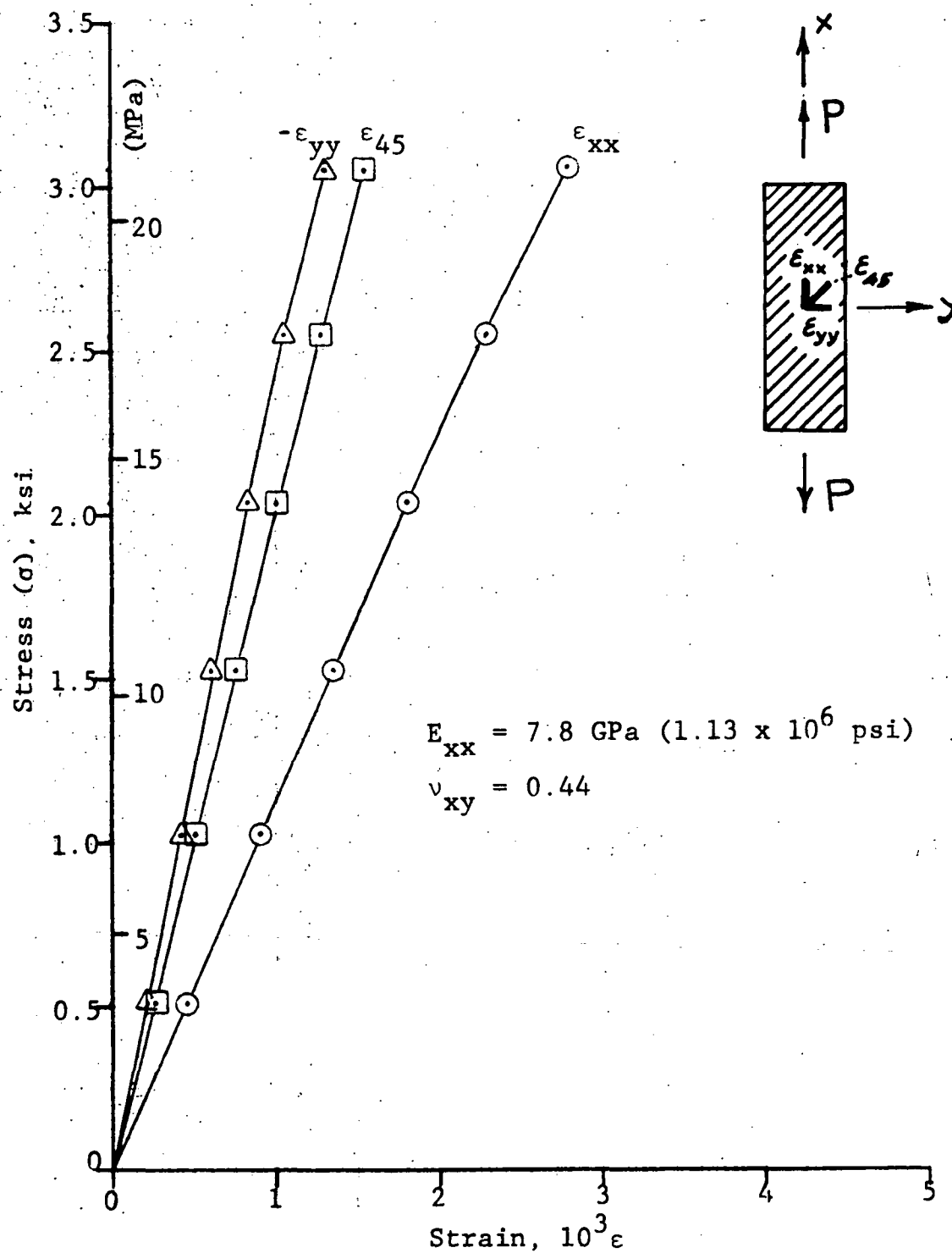


Figure 12. Stress-strain curves for $[45_{30}]$ glass/Maraset composite under uniaxial tensile loading (Style 3733; Specimen No. 42-3).

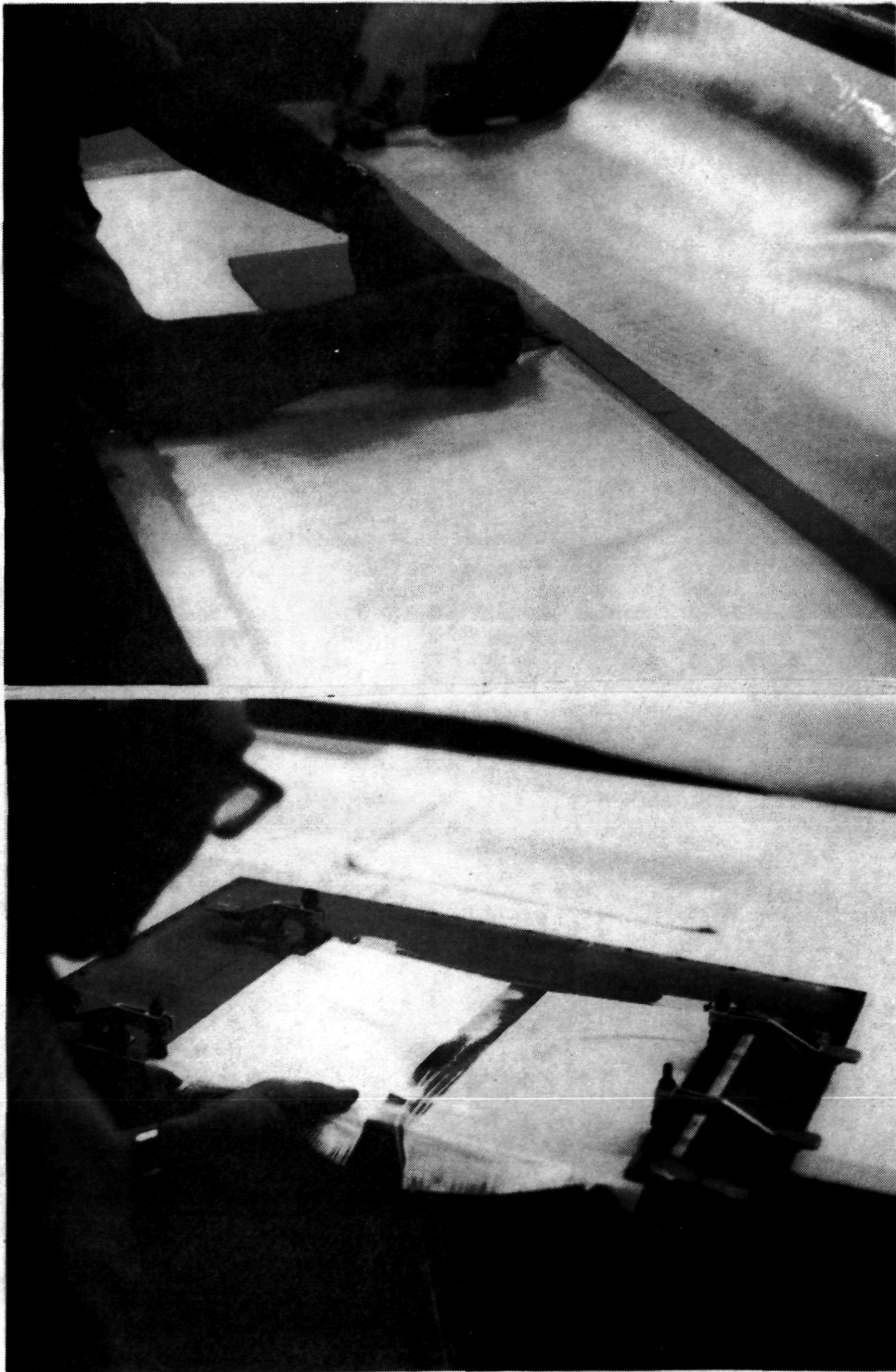


Figure 13. Cutting the glass fabric and removing fill fibers.

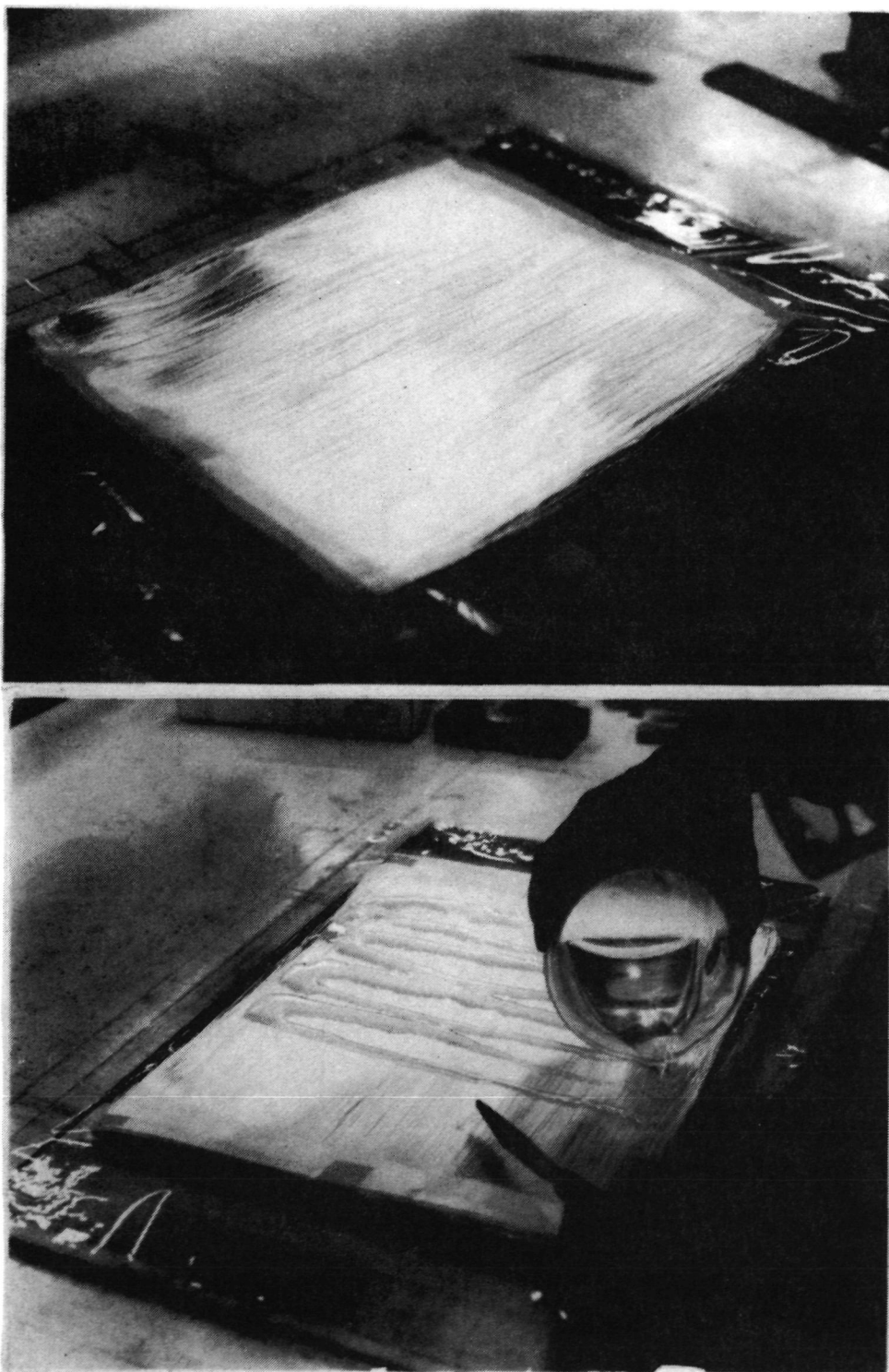


Figure 14. Placing bundles of glass fibers over teflon film and pouring resin.



Figure 15. Placing glass bleeder layers and perforated teflon film over layup.

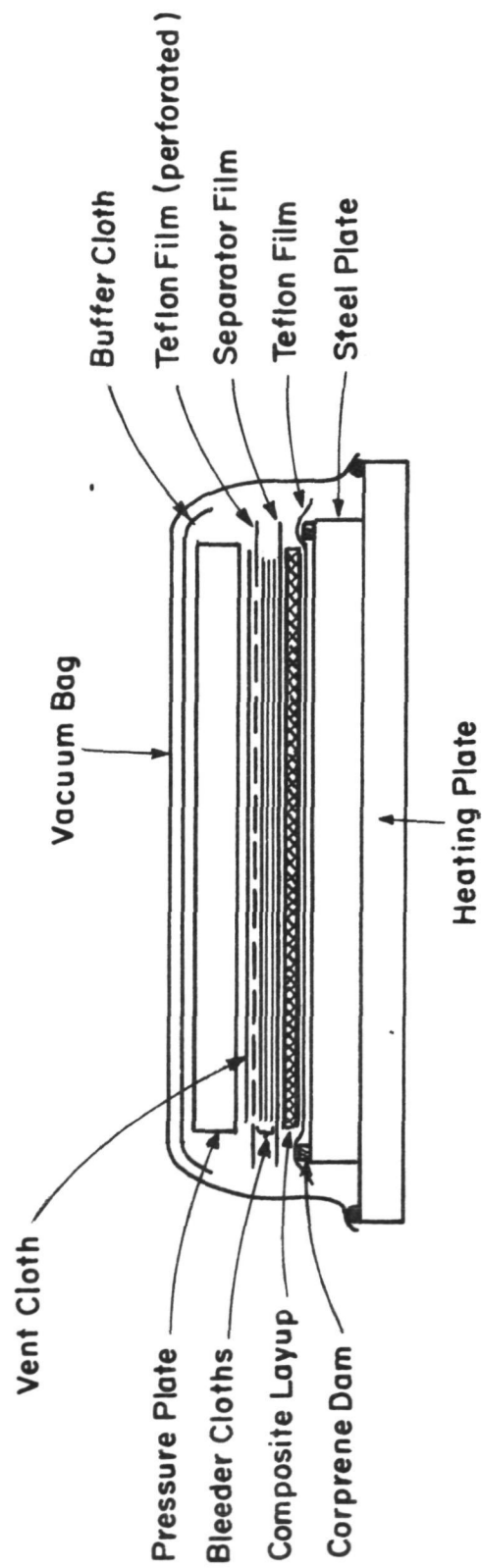


Figure 16. Sketch showing the arrangement of material layers employed in the fabrication of unidirectional birefringent laminates during the first stage of curing.

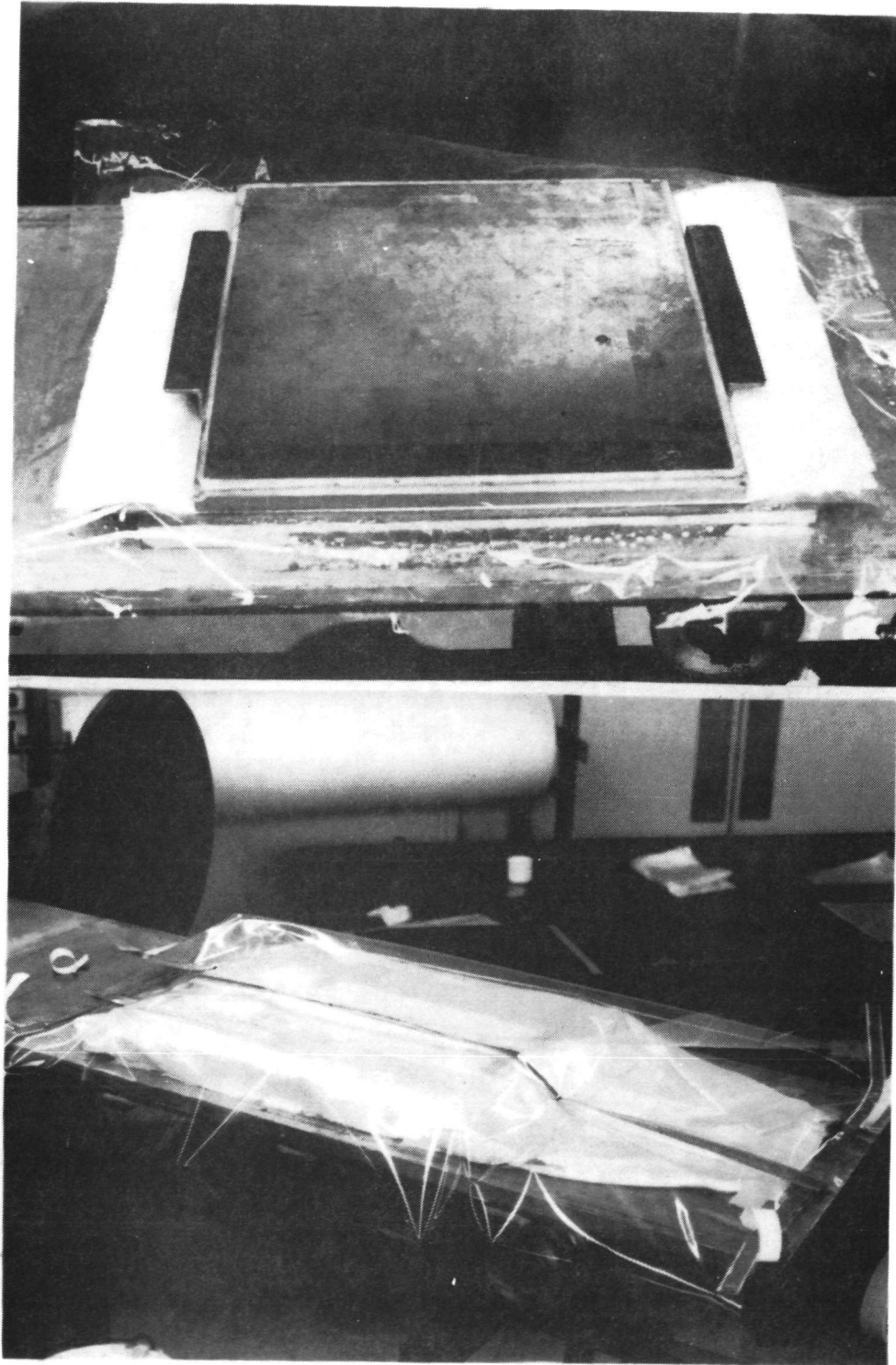


Figure 17. Composite layup with steel pressure plate and in vacuum bag before curing.

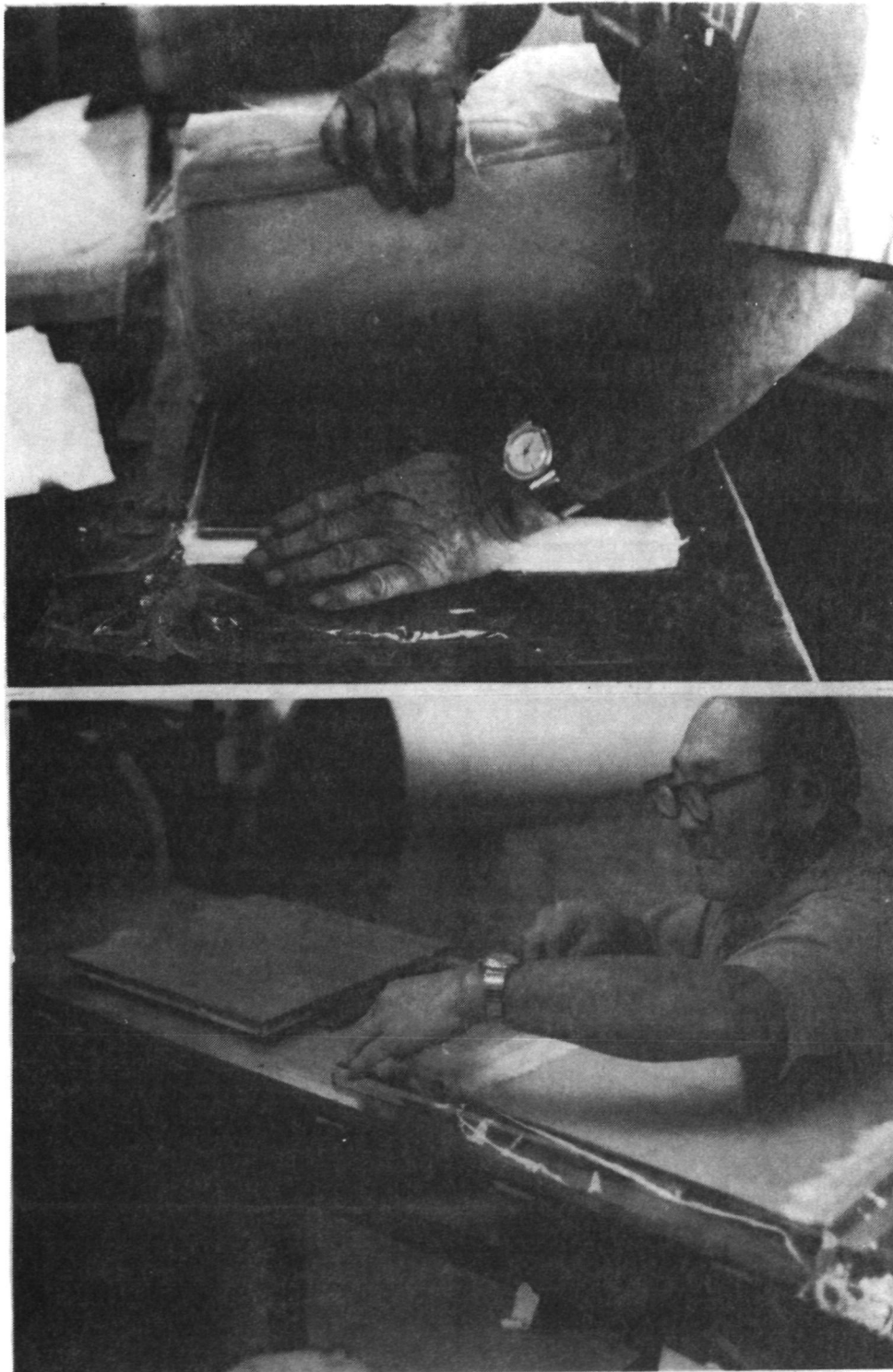


Figure 18. Removal of glass bleeder cloth after partial cure and application of teflon film.

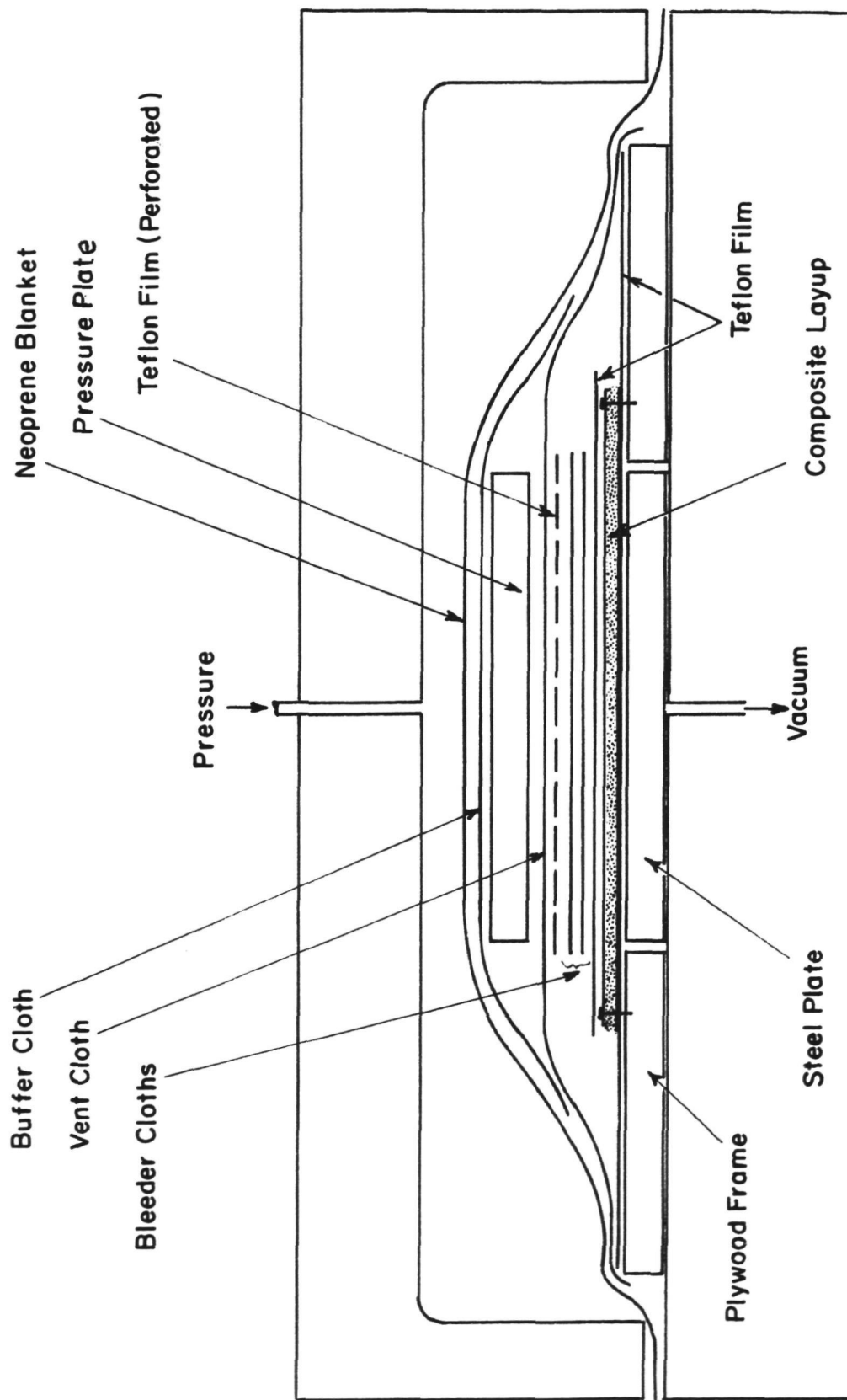


Figure 19. Sketch showing the arrangement of material layers employed in the fabrication of angle-ply birefringent composite laminates during the first stage of curing.

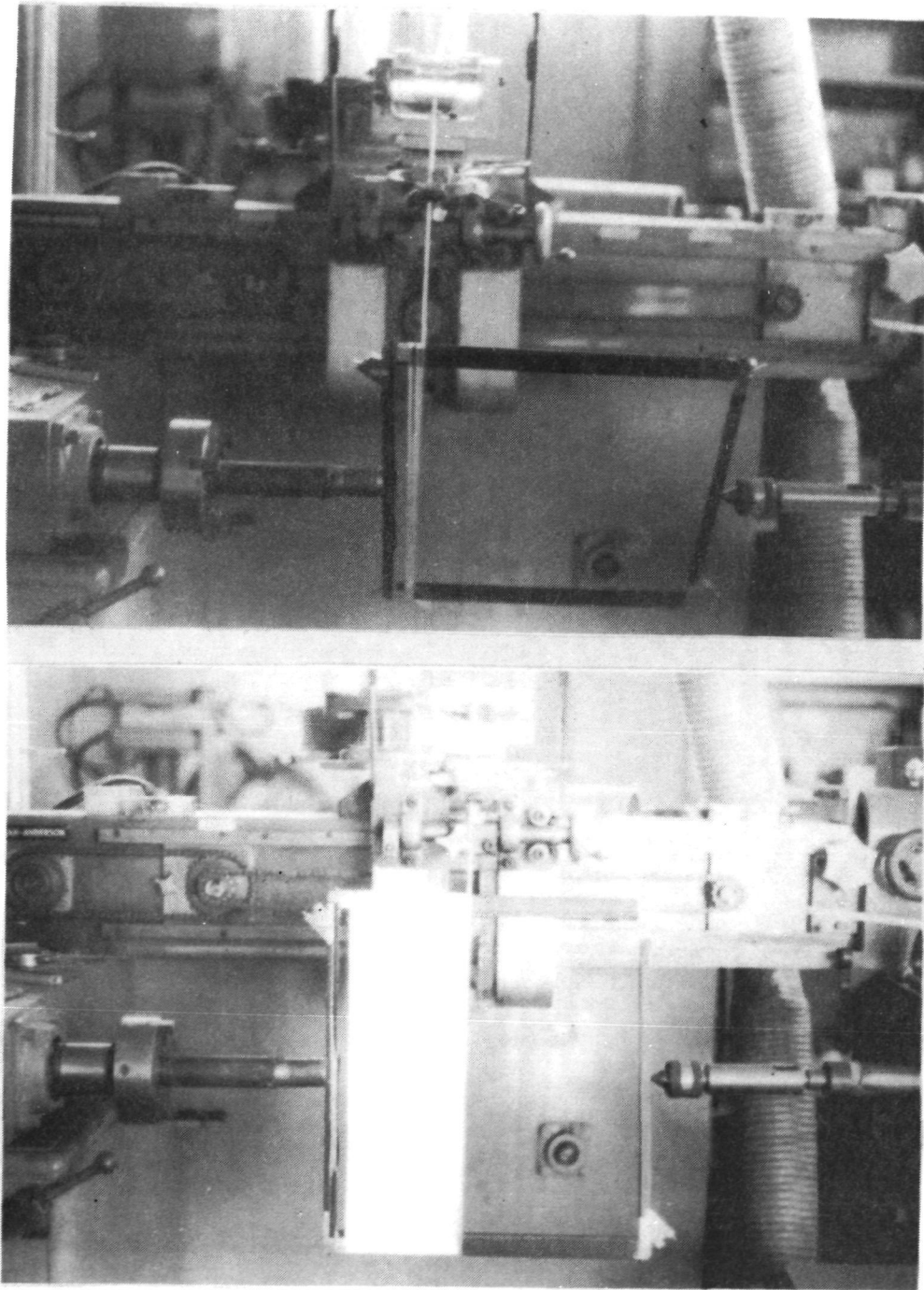


Figure 20. Winding of glass roving over a single frame for unidirectional laminates.

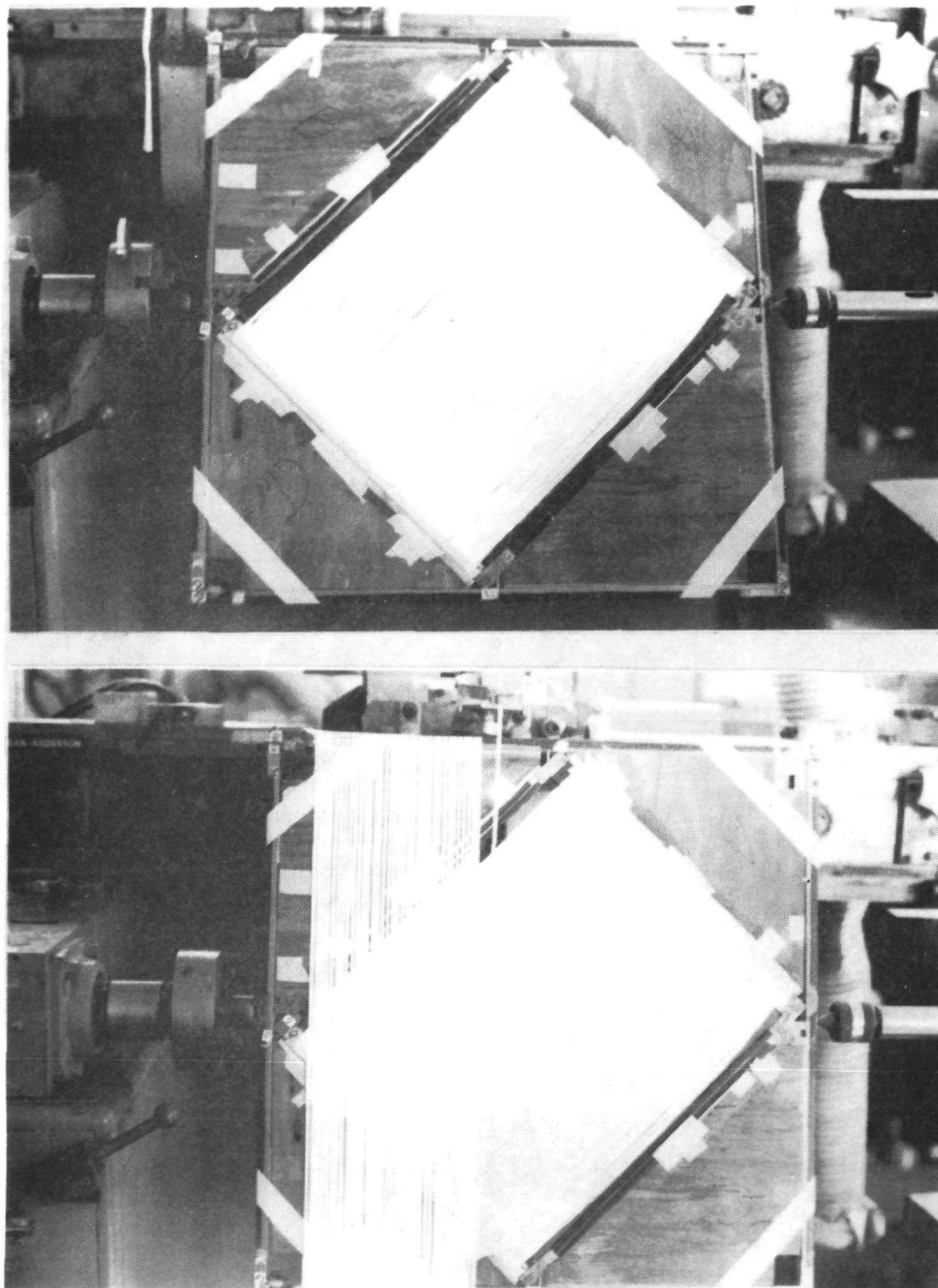


Figure 21. Mounting of frame with 90-deg plies inside large frame and winding of 45-deg plies.

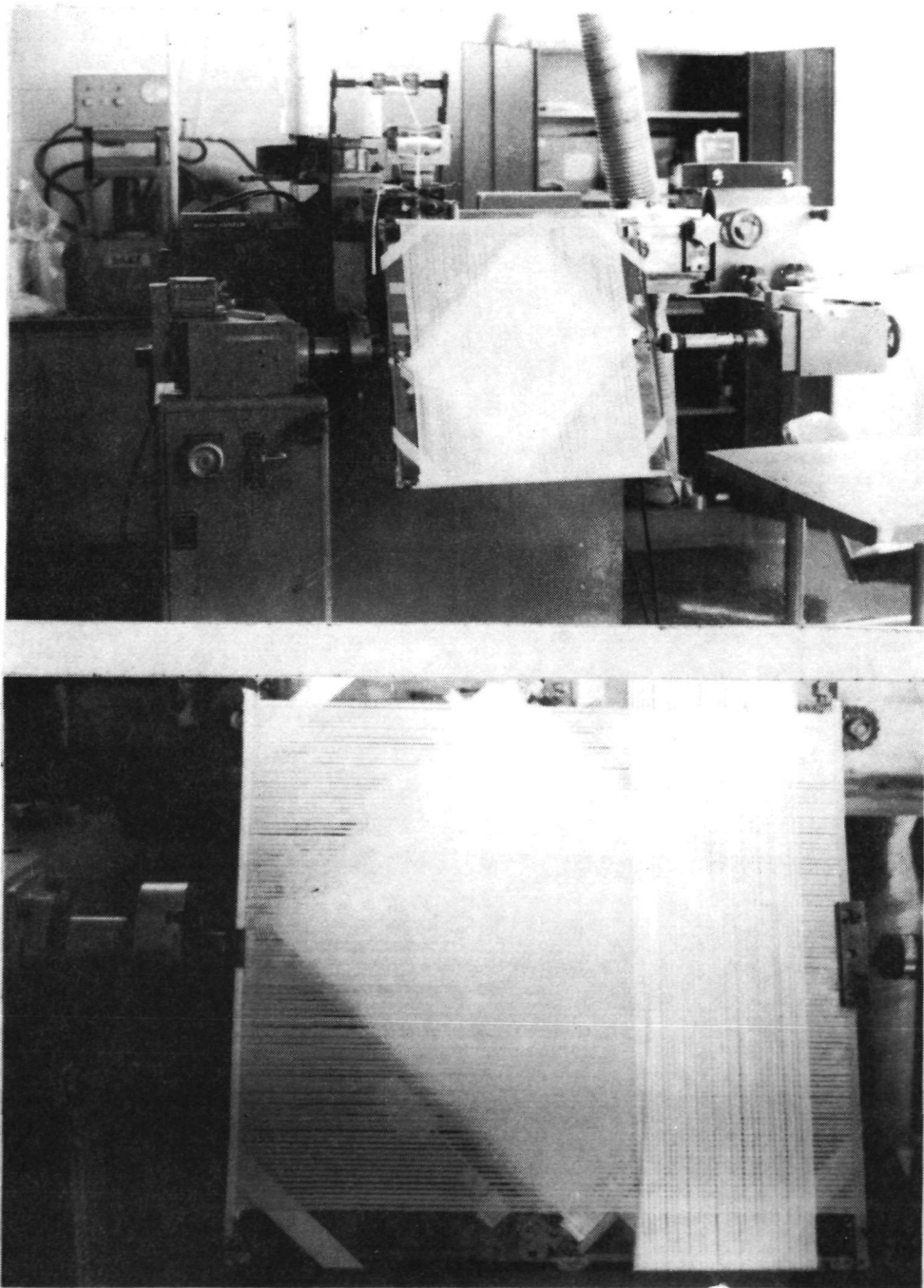


Figure 22. Winding of -45-deg plies over +45-deg and 90-deg plies.

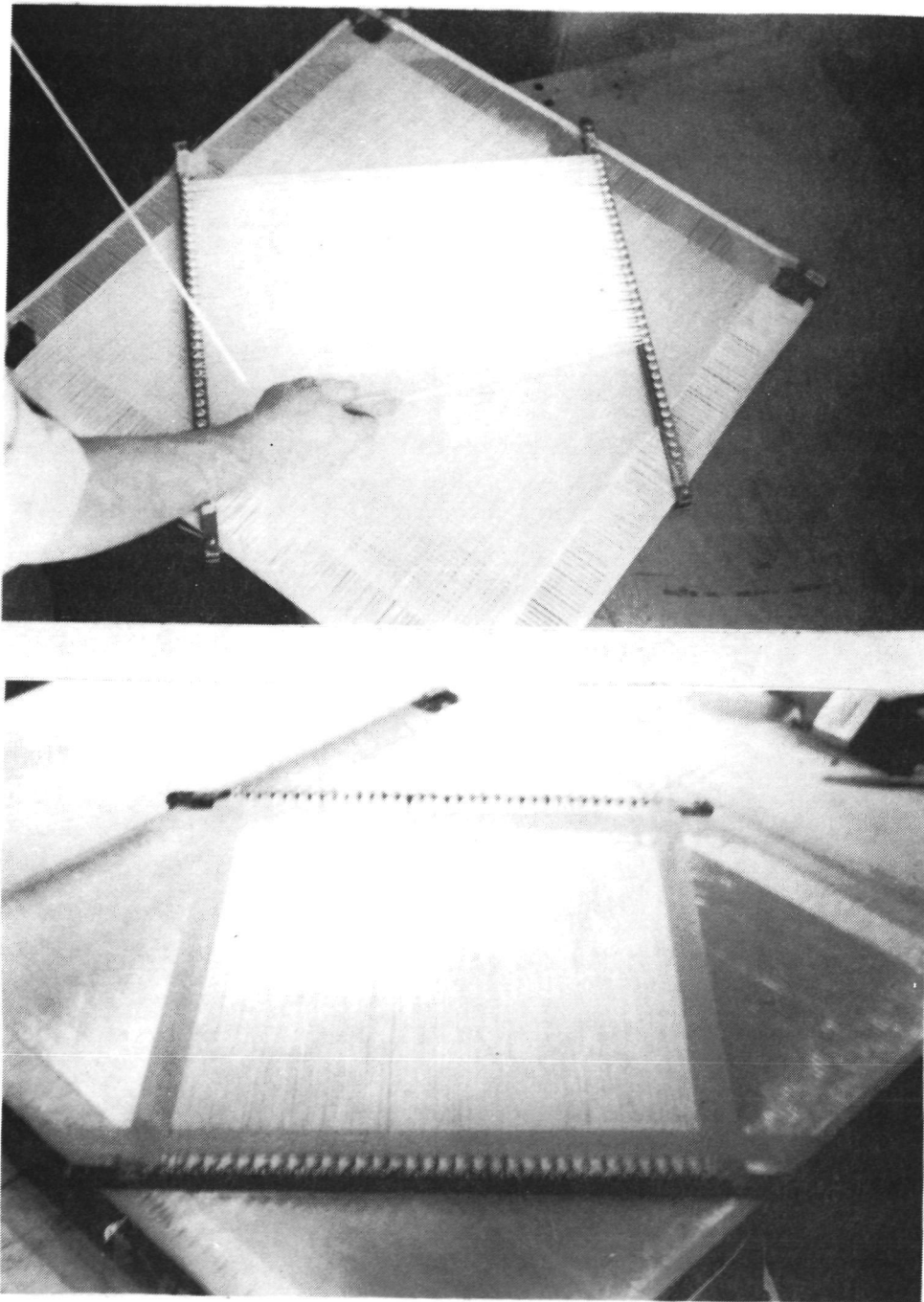
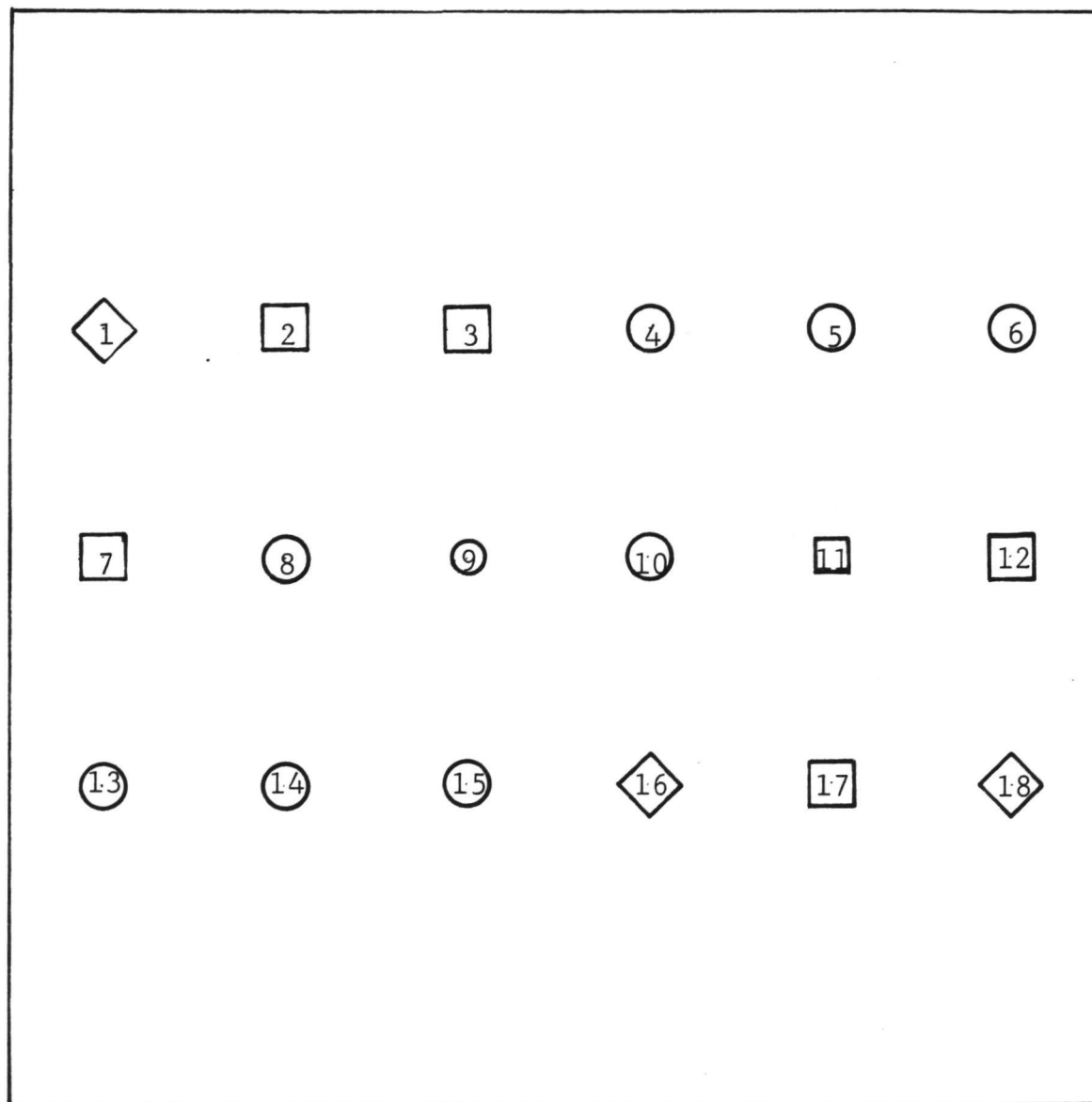


Figure 23. Threading of glass roving around screw posts for outer 0-deg plies.



<u>Inclusion</u>	<u>Material</u>	<u>Location (Plies from Top)</u>
1-6	Teflon	2
7,8,10	Kapton	2
9,11,12	Kapton	4
13-18	Teflon	4

Figure 24. Layout of embedded flaws in birefringent laminates.

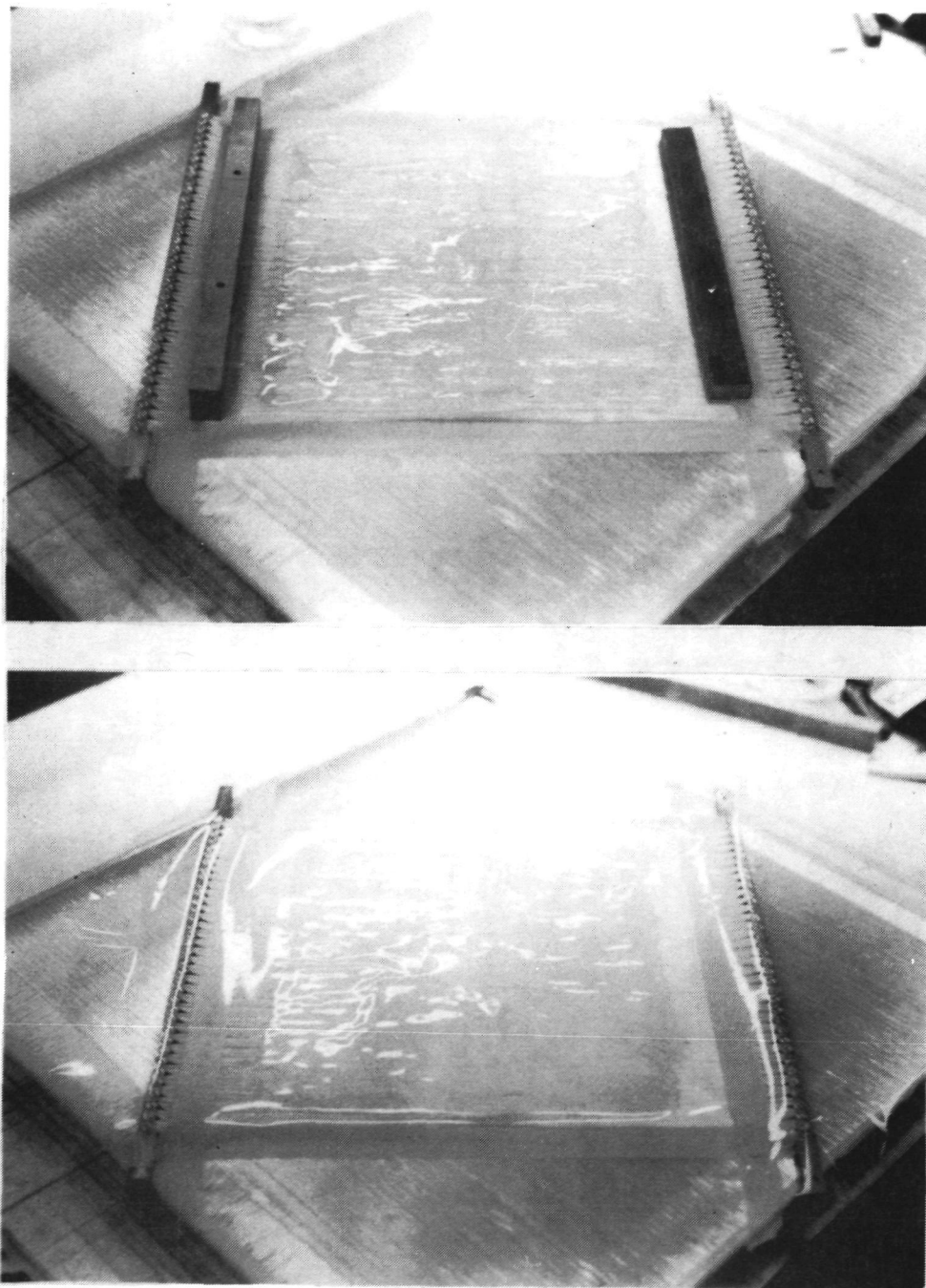


Figure 25. Winding with resin spread over it
and covered with teflon sheet.

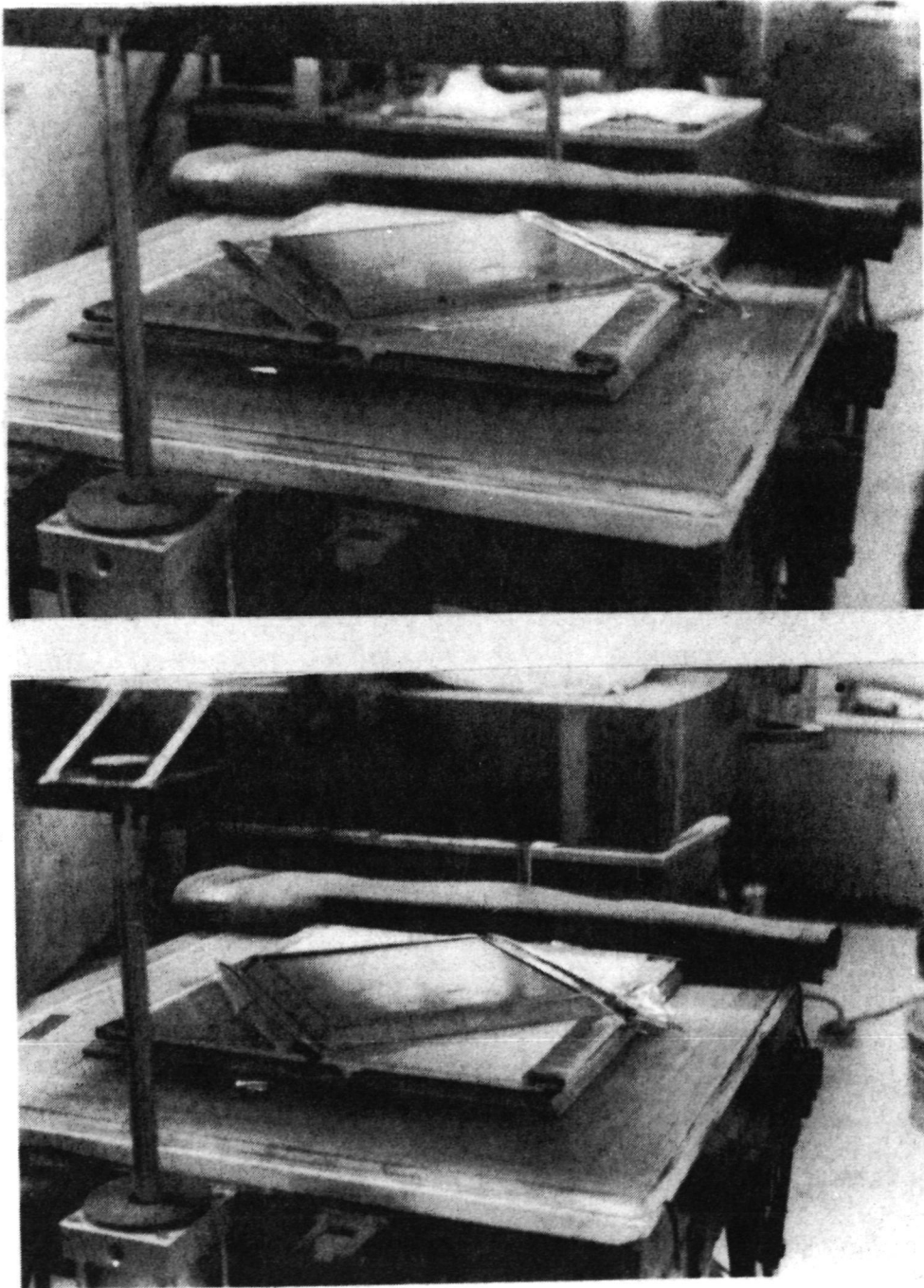


Figure 26. Layup with pressure plate in autoclave press.

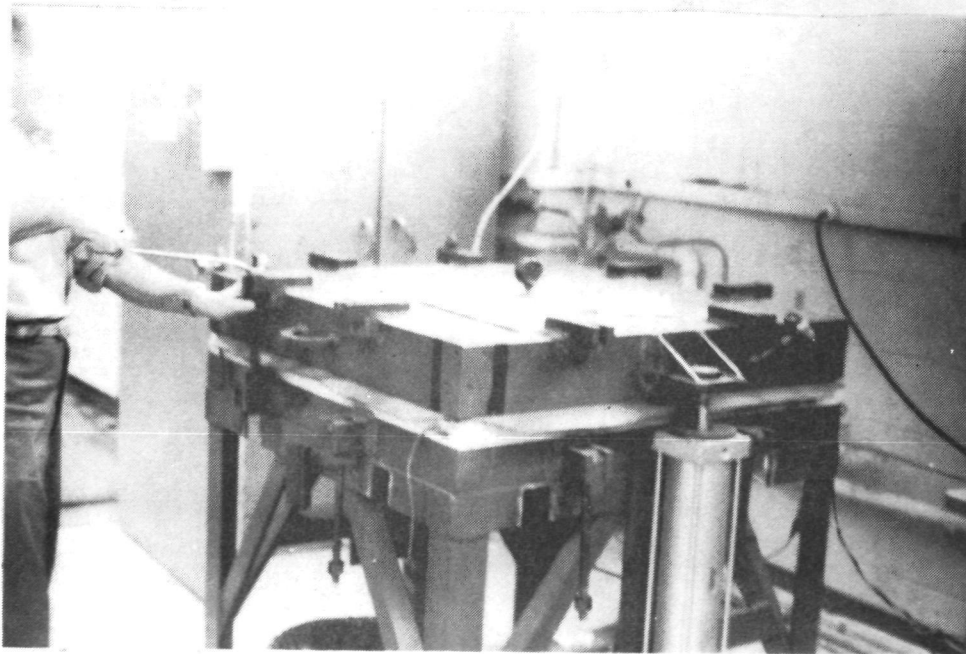
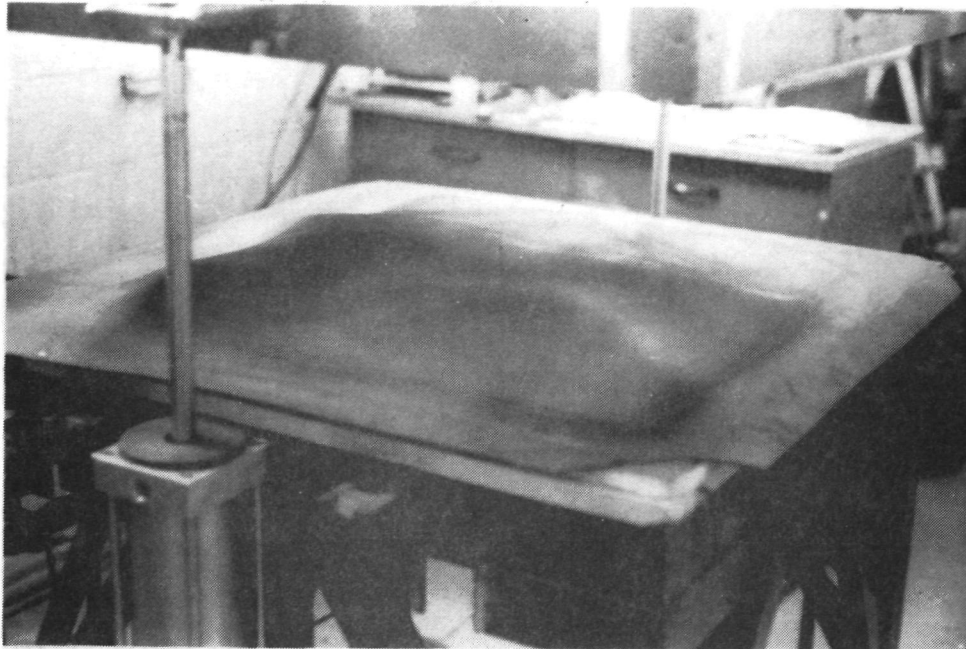


Figure 27. Curing of laminates in blanket press autoclave.

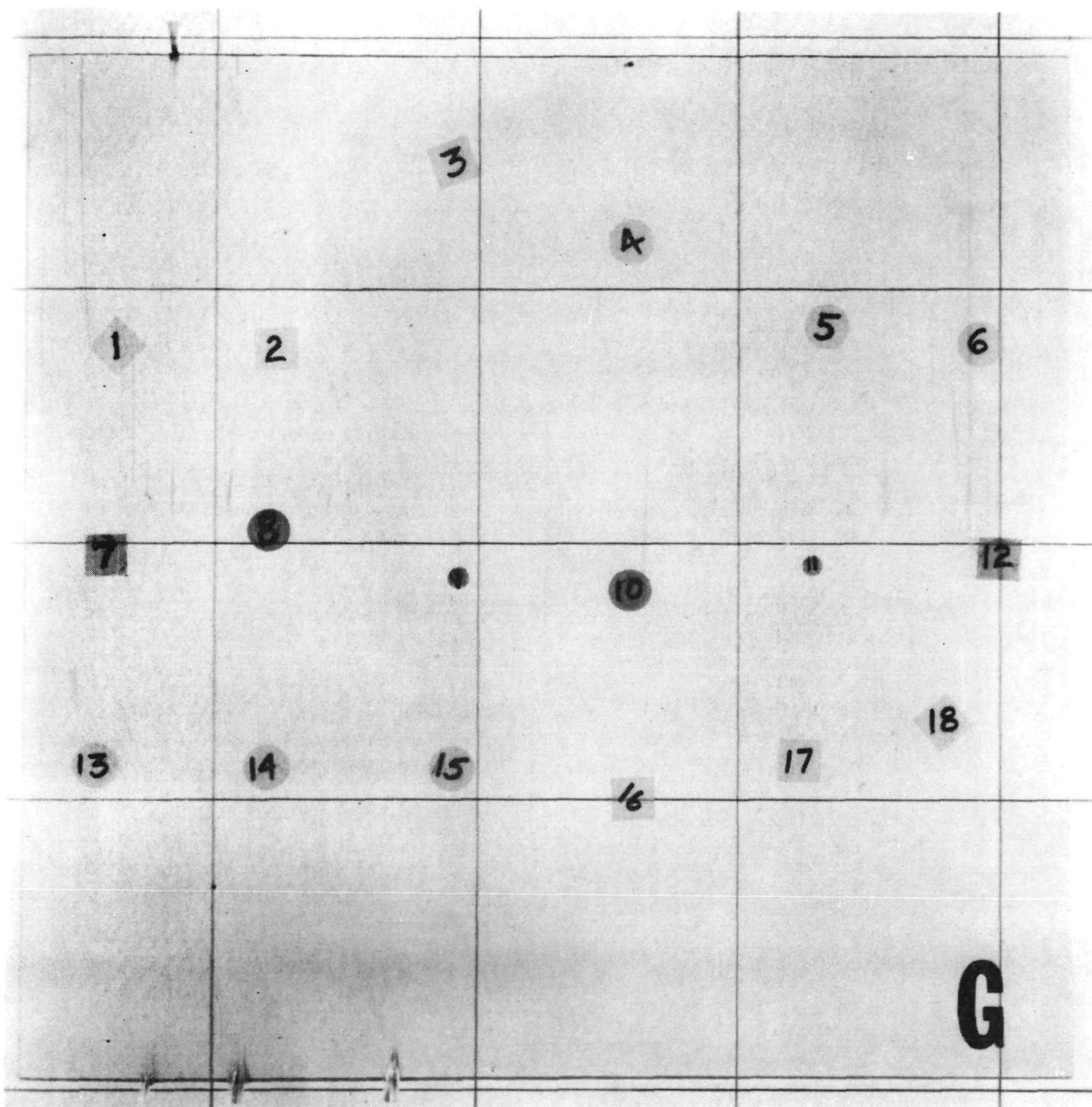


Figure 28. Unidirectional [0g] glass/epoxy plate with embedded flaws (1062 glass roving; Maraset 658/558 epoxy).

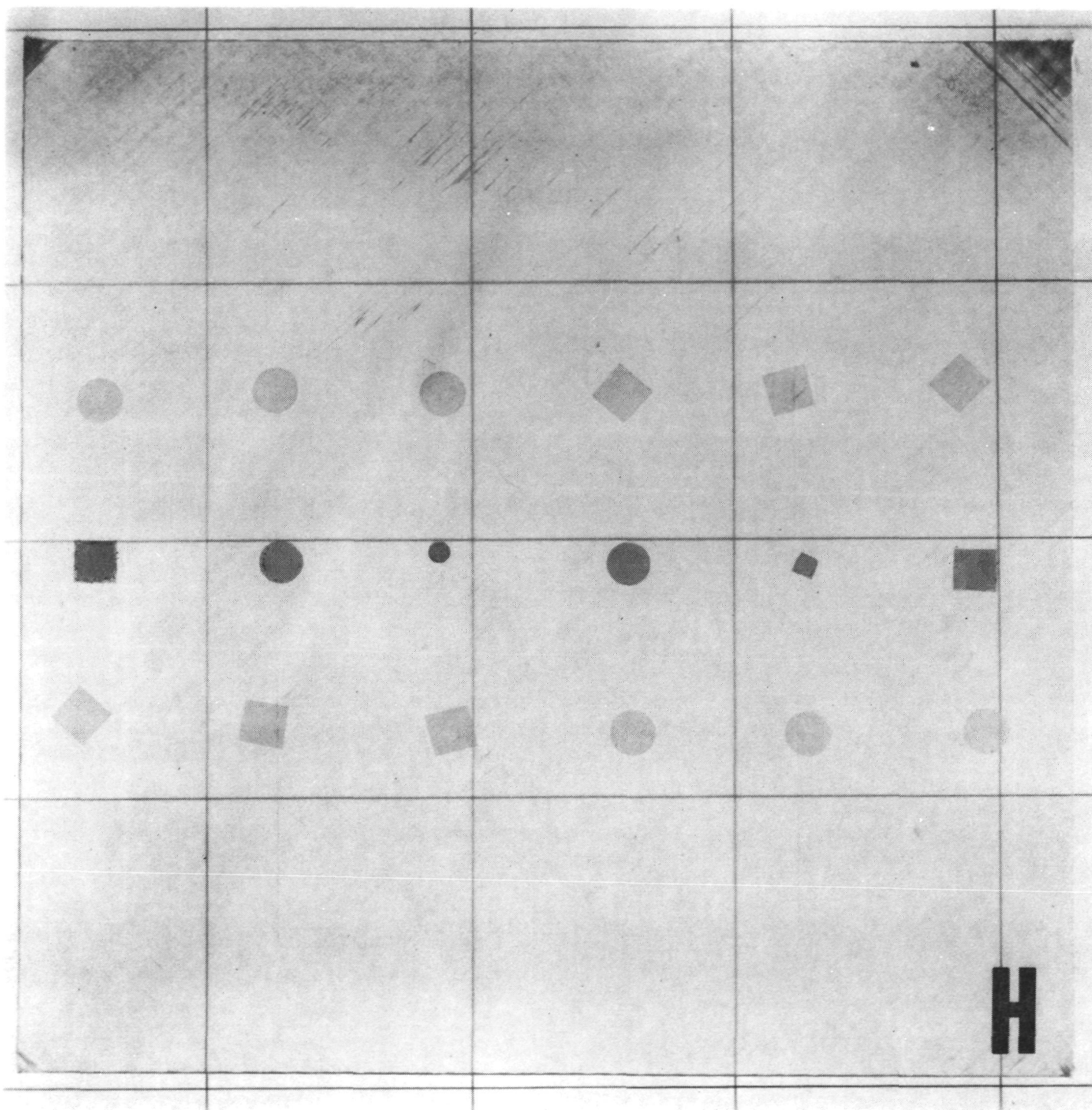


Figure 29. Angle-ply $[\pm 45]_{2s}$ glass/epoxy plate with embedded flaws (1062 glass roving; Maraset 658/558 epoxy).

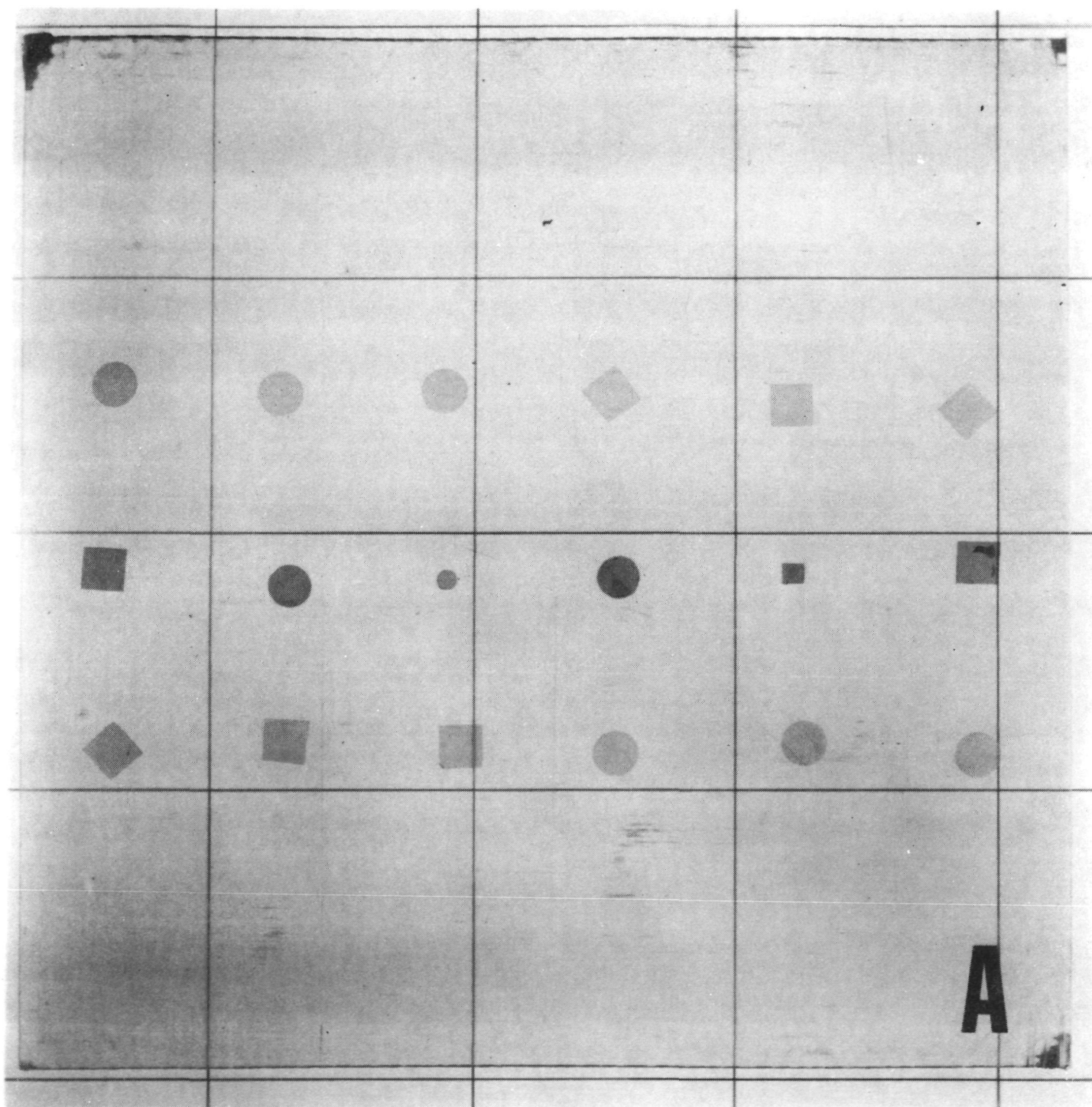


Figure 30. Quasi-isotropic $[0/\pm 45/90]_s$ glass/epoxy plate with embedded flaws (1062 glass roving; Maraset 658/558 epoxy).

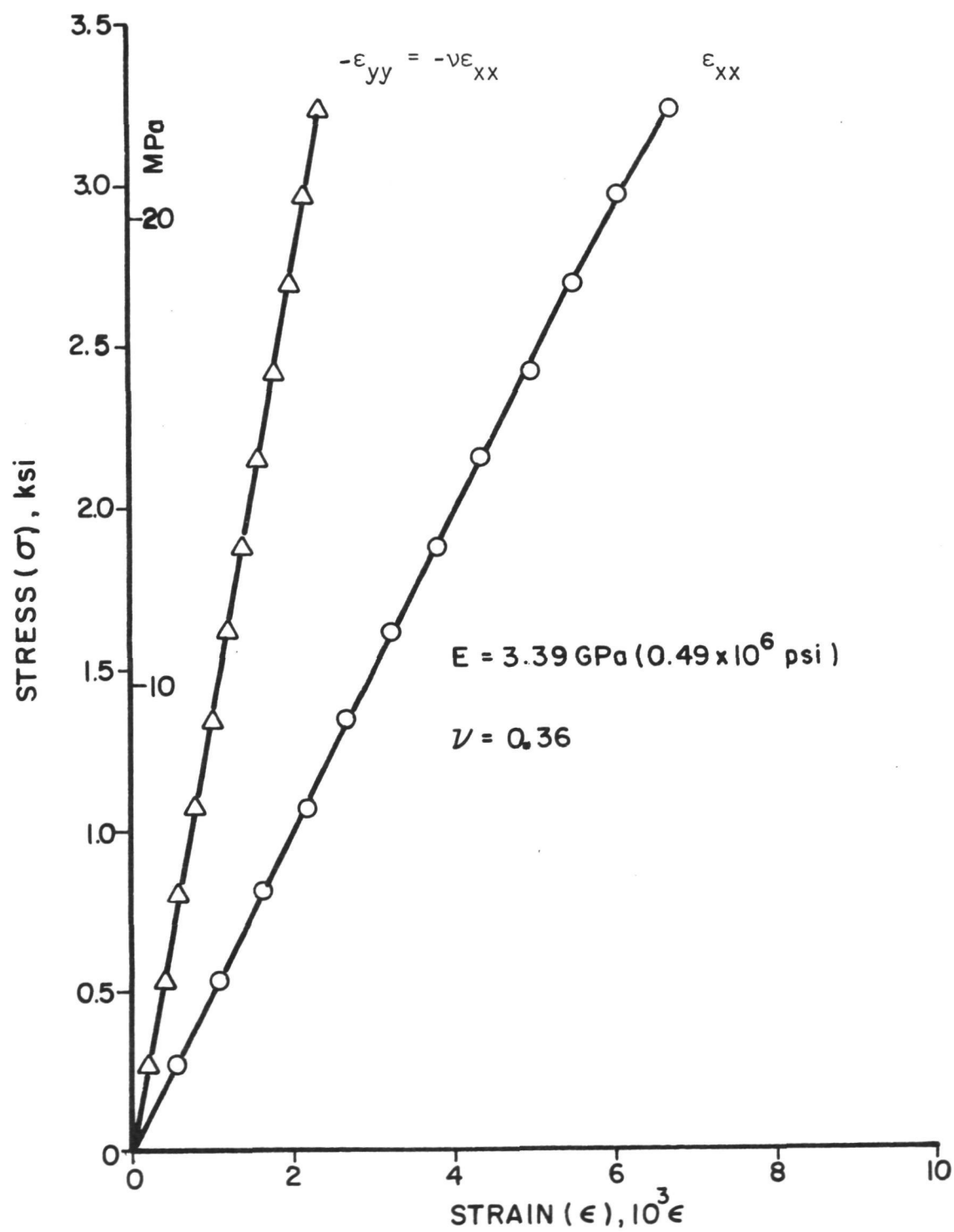


Figure 31. Stress-strain curves for Maraset 658/558 epoxy resin.

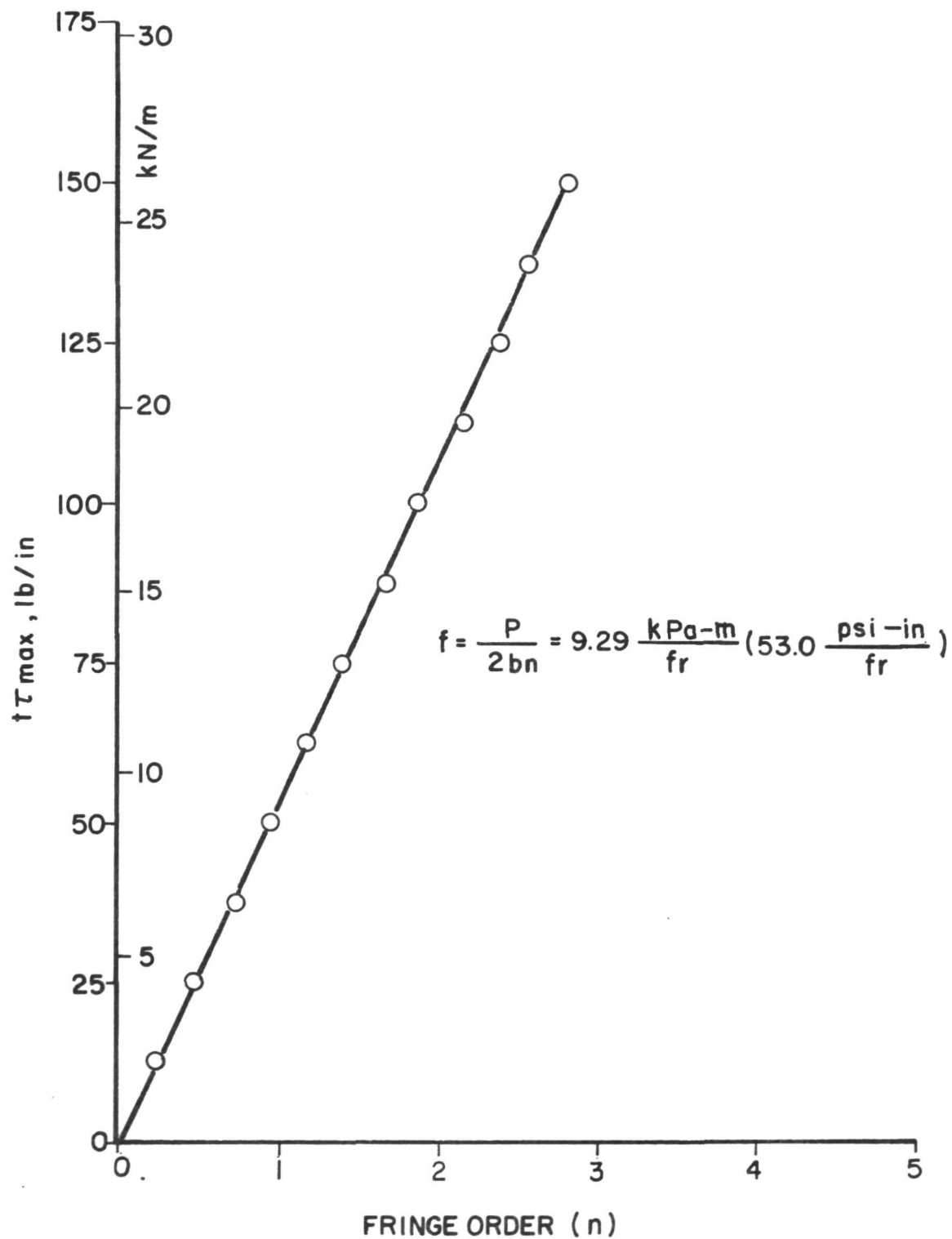


Figure 32. Stress-birefringence curve for Maraset 658/558 epoxy resin.

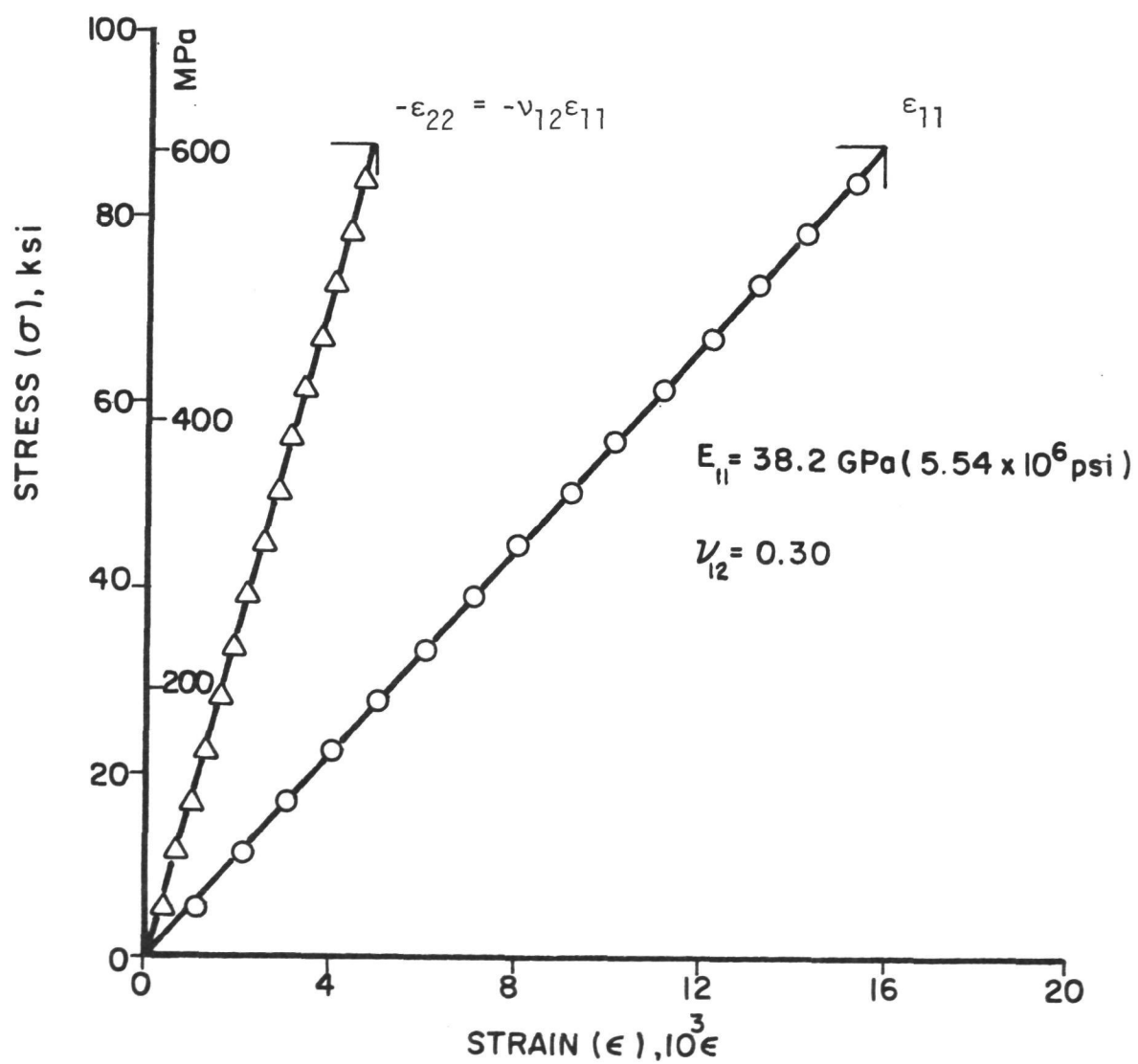


Figure 33. Stress-strain curves for $[0_{30}]$ glass/epoxy composite (Style 3733 glass; Maraset 658/558 epoxy).

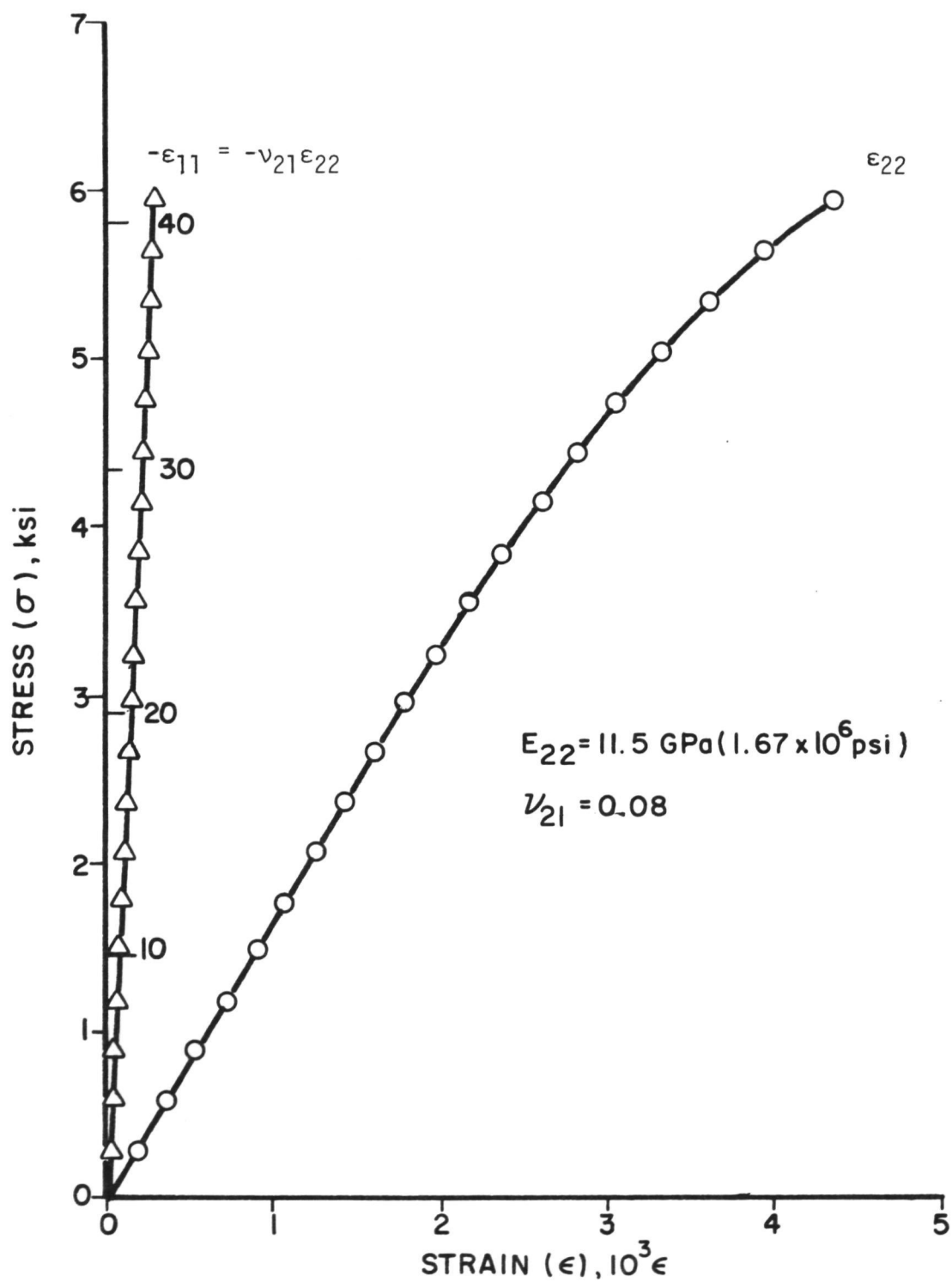


Figure 34. Stress-strain curves for $[90_{30}]$ glass/epoxy composite (Style 3733 glass; Maraset 658/558 epoxy).

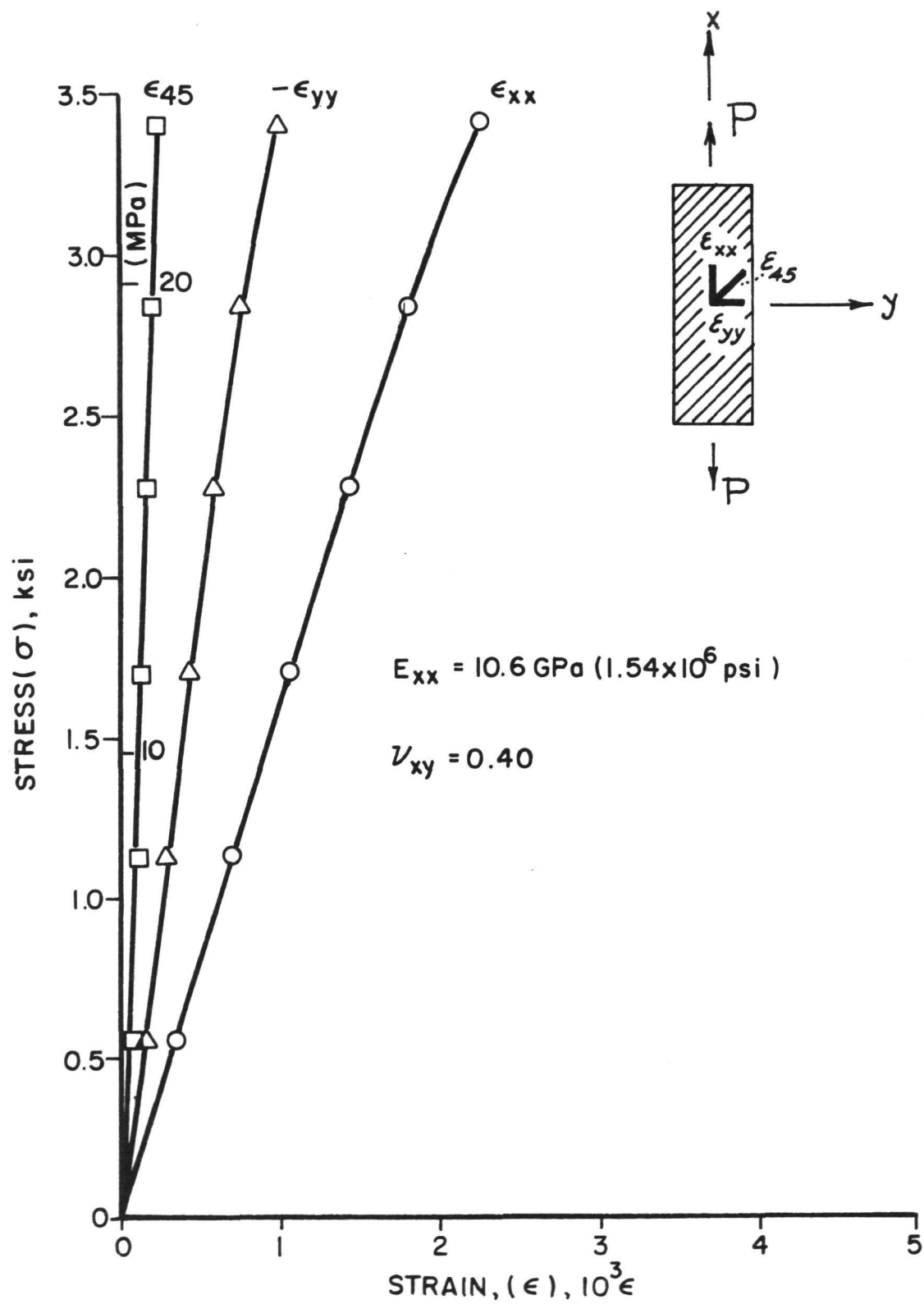


Figure 35. Stress-strain curves for $[45_{30}]$ glass/epoxy composite (Style 3733 glass; Maraset 658/558 epoxy).

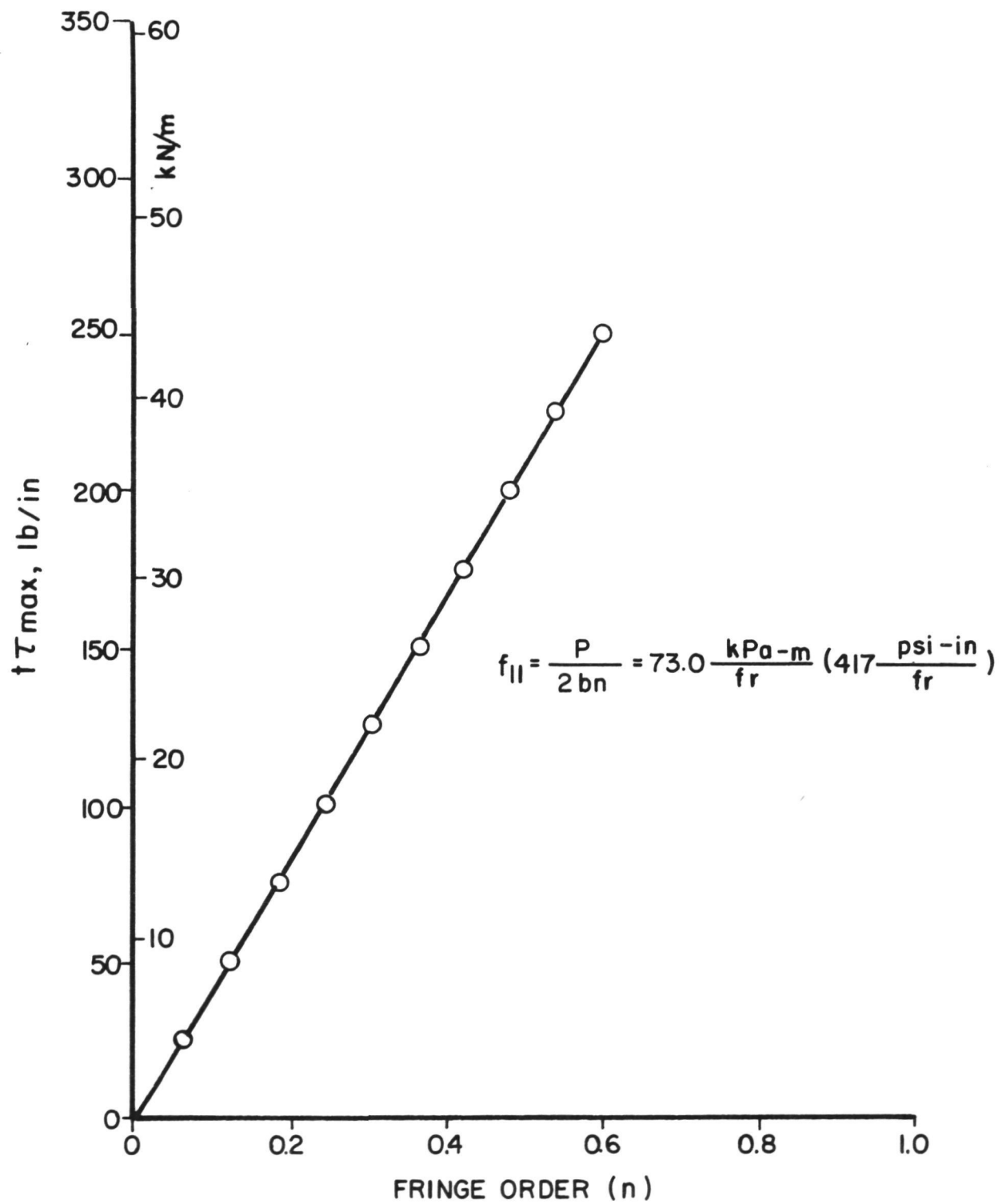


Figure 36. Stress-birefringence curve for [030] glass/epoxy composite (Style 3733 glass; Maraset 658/558 epoxy).

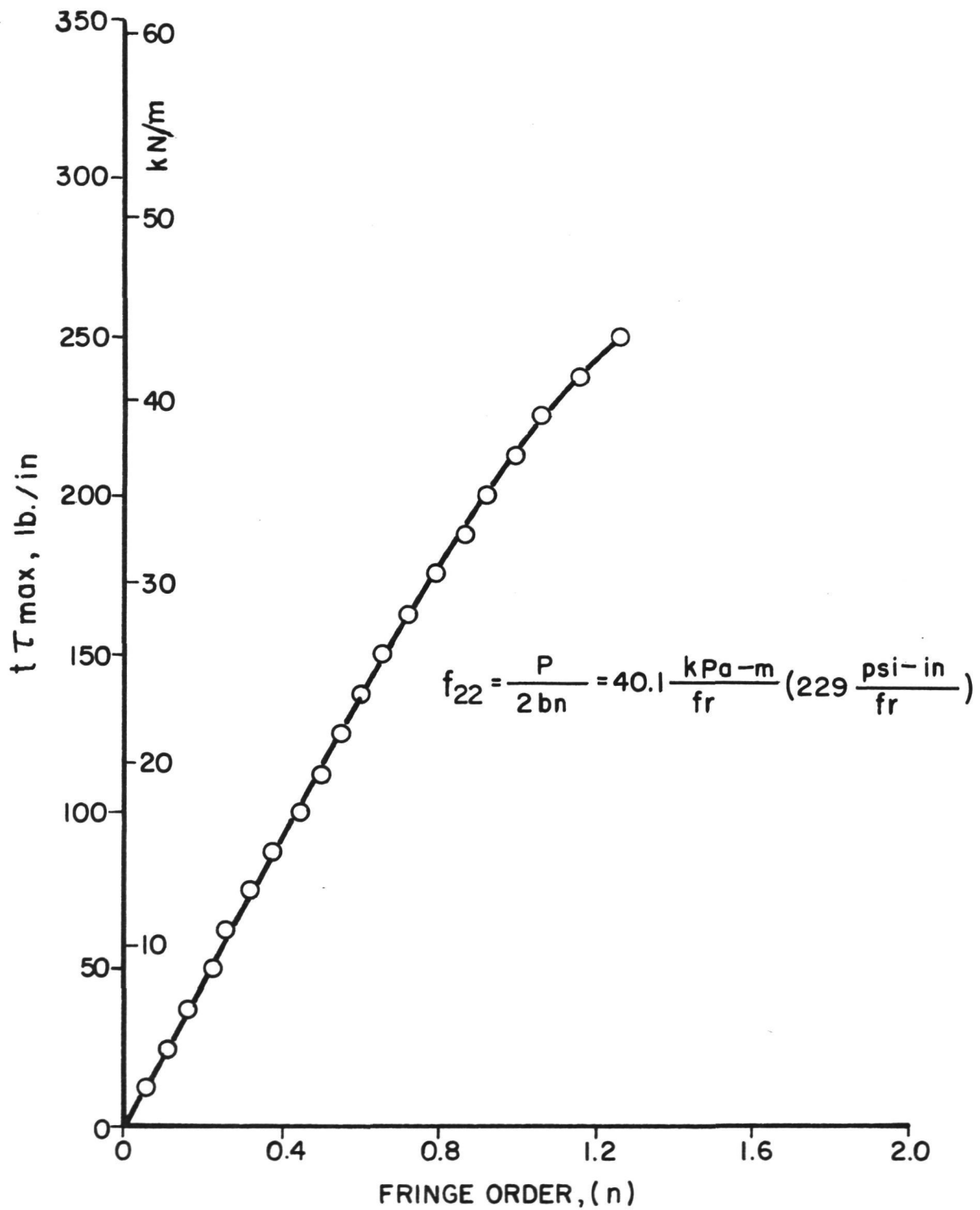


Figure 37. Stress-birefringence curve for [90₃₀] glass/epoxy composite (Style 3733 glass; Maraset 658/558 epoxy).

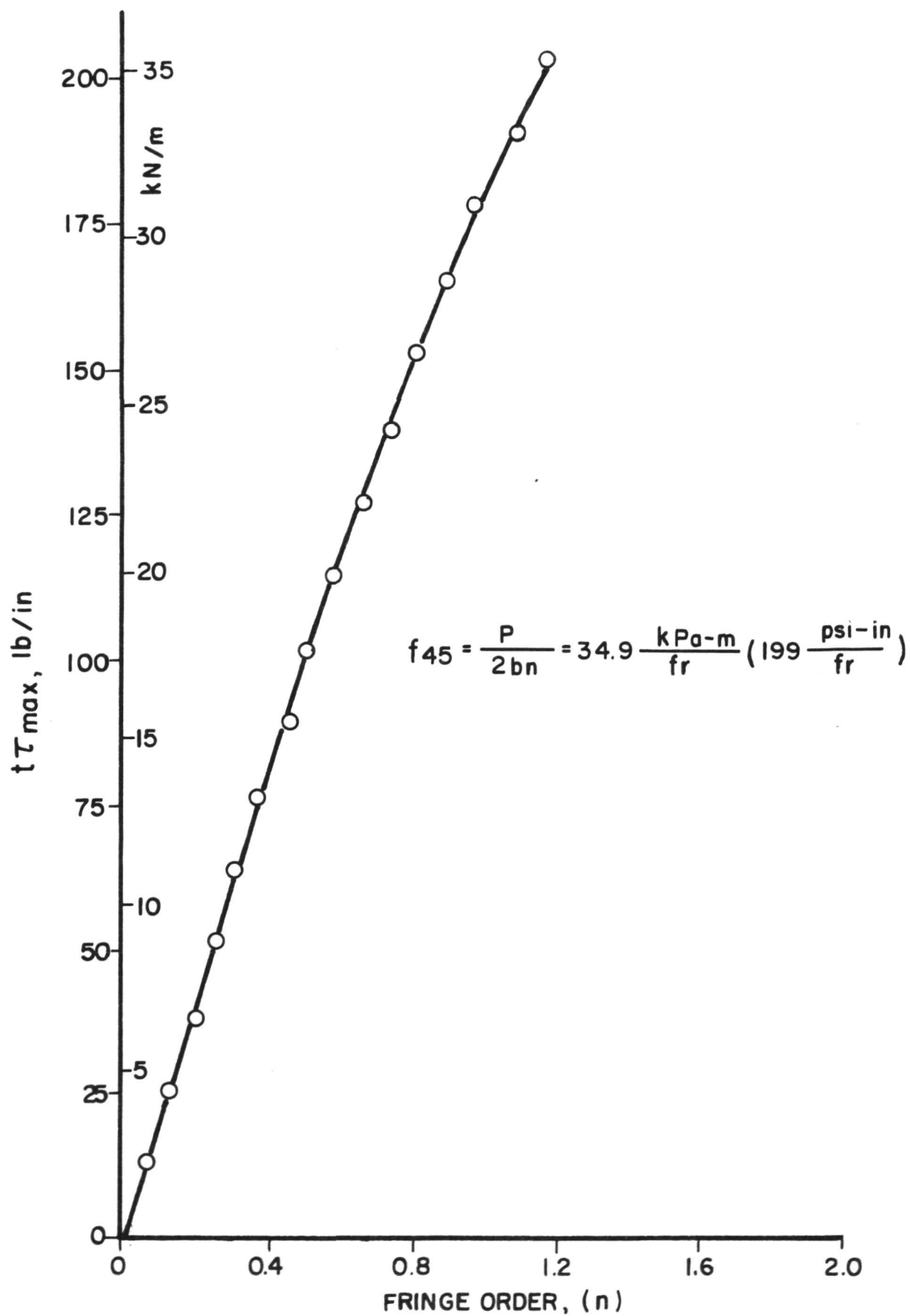


Figure 38. Stress-birefringence curve for $[45_{30}]$ glass/epoxy composite (Style 3733 glass; Maraset 658/558 epoxy).

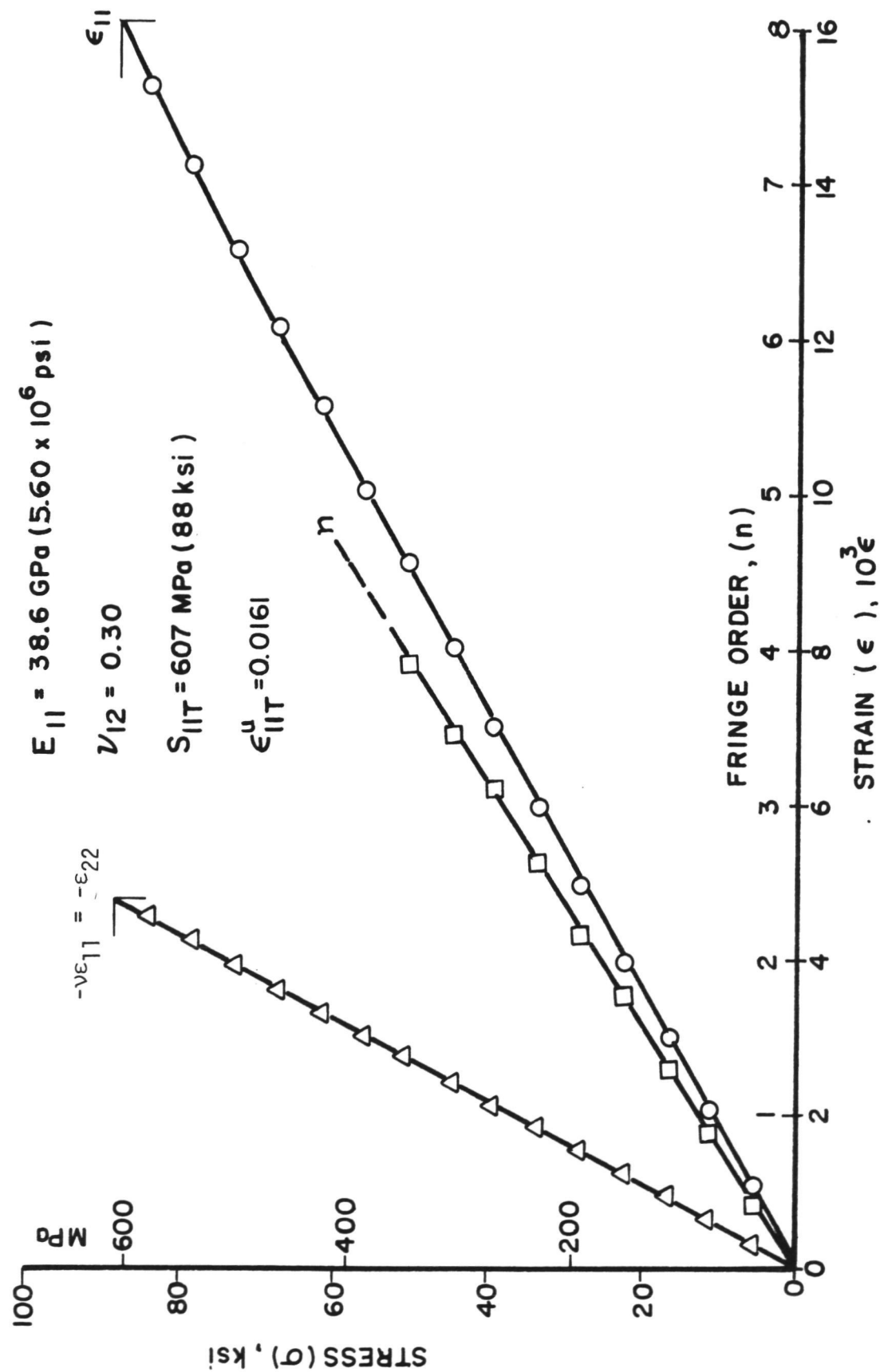
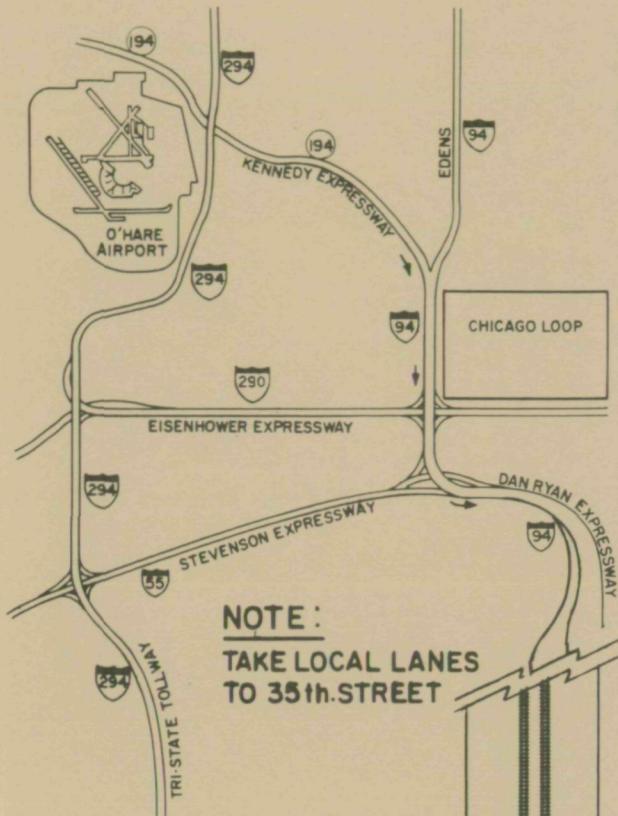


Figure 39. Stress-strain and stress-birefringence curves for $[0_{30}]$ glass/epoxy composite (Style 3733 glass; Maraset 658/558 epoxy).

HOW TO REACH
MANUFACTURING PRODUCTIVITY CENTER*



TO CHICAGO LOOP

